

Late Quaternary multi-genetic processes and products on the northern Gulf of Cadiz upper continental slope (SW Iberian Peninsula)

Thomas MESTDAGH ^{a,b,*}, Francisco J. LOBO ^c, Estefanía LLAVE ^d, F. Javier HERNÁNDEZ-MOLINA ^e, Antonio GARCÍA LEDESMA ^f, Ángel PUGA-BERNABÉU ^f, Luis-Miguel FERNÁNDEZ-SALAS ^g, David VAN ROOIJ ^a

^a Renard Centre of Marine Geology, Department of Geology, Ghent University, Krijgslaan 281 (S8), 9000 Gent, Belgium

^b Flanders Marine Institute (VLIZ), Wandelaarkaai 7, 8400 Oostende, Belgium

^c Instituto Andaluz de Ciencias de la Tierra, CSIC-Universidad de Granada, Av. de las Palmeras 4, 18100 Armilla, Spain

^d Instituto Geológico y Minero de España (IGME), Ríos Rosas 23, 28003 Madrid, Spain

^e Department of Earth Sciences, Royal Holloway University of London, Egham, Surrey TW20 0EX, UK

^f Departamento de Estratigrafía y Paleontología, Universidad de Granada, Campus de Fuentenueva, 18002 Granada, Spain

^g Instituto Español de Oceanografía, C.O. de Cádiz, Muelle de Levante s/n, Puerto Pesquero, 11006 Cádiz, Spain

(*^{*}) Corresponding author: Thomas.Mestdagh@UGent.be

Research highlights

- Significant upper-sloped morphological variability revealed off the Guadiana River
- Wide genetic diversity driven by along-/downslope processes, diapirism and gas flow
- Spatio-temporal patterns controlled by oceanographic variations and sediment supply

Keywords

Gulf of Cadiz, upper slope, plastered drift, subaqueous valley, sediment waves, sediment gravity flows

Abstract

On continental margins, the upper slope to shelf break environment forms a critical region where sediment supply, hydrographic activity and gravitational processes determine how and when sediments are partitioned between the shallow- and deep-marine realm. On the SW Iberian margin, relatively few studies have addressed the dynamics of this region, although it holds key information regarding the link between the sedimentary evolution of the continental shelf and the contourite depositional system on the middle slope. This work therefore presents a high-resolution analysis of the morphological and stratigraphic expressions of late Quaternary (dominantly last glacial and present-day interglacial) sedimentary processes on the upslope and shelf margin sector between 7° and 7°30' W.

The integration of seismic, bathymetric and hydrographic data reveals the presence of alongslope processes and products (abottom current-related plastereddrift,moat, erosional surfaceand terrace, an internal wave-/tide-controlled sediment wave field), downslope (gravitational) processes and products (an upslope – shelf marginvalleysystem, slumps, debrites,gullies), neotectonicelements (diapirs) and fluid flow features (pockmarks, bright spots). The spatial distribution of these features indicates that the study area becomes increasingly alongslope-dominated towards the W, and oppositely, more downslope-dominated towards the E, because sediment supply to the latter area is enhanced under the dominant eastward dispersal of fluvially supplied sediments on the shelf. In addition, glacial-interglacial variations in the amount of sediments supplied to the shelf edge and the intensity of oceanographic processes in the study area also generate a distinct temporal variability, with glacial and interglacial intervals respectively recording principally downslope- and alongslope-controlled morphological elements. Finally, regardless of these overall spatial and temporal patterns, diapirism and fluid flow are inferred to locally destabilize sediments and induce small-scale mass wasting in the study area. These findings are not only relevant to the northern Gulf of Cadiz, but also to the general understanding of sedimentary dynamics and controls in mixed downslope- and alongslope-controlled upslope to shelf margin settings worldwide.

1. Introduction

The shelf break to upper slope domain constitutes a key environment where sediment partitioning and process interaction between the shallow- and deep-water realm take place (Kennett, 1982; Shanmugam, 2006; Pickering and Hiscott, 2016). Sediment transport and deposition processes at the shelf edge are influenced by a number of geological and environmental factors acting at different timescales (Karl et al., 1983). At long timescales (i.e. millions of years), the overall shelf break progradation is determined by the geological setting of the margin, driving tectonic deformation and the subsidence pattern (Pratson et al., 2007). These tectonic processes interact with eustatic sea-level changes (Mougenot et al., 1983; Pitman and Golovchenko, 1983; Vanney and Stanley, 1983), which may influence shelf-margin sedimentary processes through shelf subaerial exposure and shoreline deposition (Pratson et al., 2007).

At shorter timescales, the shelf margin is mainly influenced by the amount and nature of sediment supply (Vanney and Stanley, 1983) and distributive hydrodynamic processes such as waves, tides and currents (Field et al., 1983). High depositional rates induce downslope depositional and erosional processes and a variety of mass movements leading to shelf edge progradation and/or development of submarine conduits (Coleman et al., 1983). In gently sloping margins, the major sediment suppliers are rivers that generate major shelf-margin deltas characterized by a typical clinoform geometry (Porębski and Steel, 2003). They evolved downslope into sedimentary wedges, which comprise a variety of deposits such as prodeltas, mud belts and (hemi)pelagic deposits that are genetically related to low-density turbidity currents (Prather et al., 2017). Sediment gravity flows caused by oversteepening and high accumulation rates enhance the sediment transfer towards deeper domains (Coleman et al., 1983; Steel et al., 2008). These mass movements may shape different types of submarine valleys (Pratson et al., 2007), particularly in high gradient settings, even under conditions of moderate sediment supply (O'Grady et al., 2000).

In low supply margins, the sediment transfer towards the deep basin and the development of deep turbidite systems are more directly controlled by the sea-level trends (Pitman and Golovchenko, 1983;

Steel et al., 2008). In addition, alongslope (bottom current-controlled) processes and products have become increasingly recognized as an essential element in continental slope systems (Hernández-Molina et al., 2008; Rebesco et al., 2014), and can produce considerable lateral (along-strike) variability in their morpho-sedimentary and -stratigraphic expressions (Brackenridge et al., 2011). Although traditionally studied in deeper waters, a number of oceanographic processes may exert a considerable influence at the shelf break, including water mass fronts, thermohaline boundary currents, cascading currents, wind-driven currents, tides and internal/surface waves (Karl et al., 1983; Verdicchio and Trincardi, 2008). These processes may establish an equilibrium depth for the shelf break due to their control over erosion and sediment distribution (Mougenot et al., 1983), and give way to a wide array of deposits ranging from small-scale sandy bedforms to (shallow-water) mud-dominated contourite drifts (Verdicchio and Trincardi, 2008), generating convex-up shelf-margin profiles (Adams and Schlager, 2000).

Over the past decades, the northern Gulf of Cadiz continental margin has been the focus of numerous morphologic and stratigraphic studies. These studies mostly centered on the evolutionary patterns of either the continental shelf, mostly driven by late Quaternary sea-level changes (Somoza et al., 1997; Rodero et al., 1999; Hernández-Molina et al., 2000; Hernández-Molina et al., 2002; Lobo et al., 2005), or of the middle slope contourite depositional system (CDS), which has developed under the action of the Mediterranean Outflow Water (MOW) (Nelson et al., 1993; Hernández-Molina et al., 2006; Llave et al., 2007; Marchès et al., 2007; Llave et al., 2011; Roque et al., 2012; Hernández-Molina et al., 2016a). Yet, the link between these two continental margin domains, i.e. the upper continental slope, has received relatively little attention (Mestdagh et al., 2019).

Previous studies on the northern Gulf of Cadiz upper slope have described a wide genetic diversity of morphological elements. The most significant morphologies and deposits include shelf-margin deltas favored by sediment supply from major rivers like the Guadiana and Guadalquivir (Rodero et al., 1999; Lobo et al., 2005), and sediment drifts (plastered and mixed drifts), which are likely related to bottom

current-activity at the boundary between the northern part of the CDS and the upslope (Llave et al., 2007; Brackenridge et al., 2019; Mestdagh et al., 2019). Besides, erosional (e.g. gullies, erosional surfaces), gravitational (slides, slumps and creep), neo-tectonic (e.g. diapirs, faults) and fluid flow features (pockmarks, gas-charged sediments) have been described as well, mostly in the eastern sector of the upslope close to the Strait of Gibraltar (Baraza and Ercilla, 1996; Baraza et al., 1999; Lee and Baraza, 1999; Nelson et al., 1999; Casas et al., 2003; Medialdea et al., 2009). In addition, some morphological elements have been ascribed to different genetic processes. For example, undulating bedforms were initially interpreted as slump zones resulting from post-depositional sediment failure (Baraza et al., 1999), but were later suggested to be depositional sediment waves instead, formed under the action of downslope turbidity currents (Lee et al., 2002).

Recent high-resolution reflection seismic profiles acquired over the central to western sector of the northern Gulf of Cadiz upper slope (off the Guadiana River) now provide the opportunity to reassess and expand the inventory of aforementioned along- and downslope upper slope morphological features. Importantly, these profiles encompass a revised and dated late Quaternary stratigraphic framework, through the connection with IODP Expedition 339 sites U1386 and U1387 on the middle slope (Mestdagh et al., 2019). The study area furthermore exhibits lateral gradients in the main controlling factors driving shelf break to upper slope sedimentary processes. For example, fluvial supply is highest in the central sector of the margin between the Guadalquivir and Guadiana rivers, and is drastically reduced towards the west off the Algarve Shelf (Lobo et al., 2004), whereas the interaction of oceanographic processes with the upper slope may also show significant lateral variations (Stow et al., 2009). Hence, based on the seismic dataset complemented with additional oceanographic and bathymetric information, the aims of this study are to (i) identify and characterize the various morphological and stratigraphic expressions of late Quaternary sedimentary processes on the shelf margin and upper slope off the Guadiana River (between 7° and 7°30' W), (ii) infer the underlying formation mechanism(s) of the different sedimentary products, and (iii) evaluate the spatial and (through the stratigraphic framework) temporal variation in the identified processes and products,

with a dominant focus on the last glacial and present-day interglacial intervals. As such, the presented case attempts to enhance the general understanding and characterization of sedimentation in shelf margin – upperslope domains wheredown- and alongslope processes interactand/oralternate.

2. Study area

2.1. Geological setting

The late Cenozoic geological evolution of the Gulf of Cadiz is dominated by the convergence between Eurasia (Iberia sub-plate) and Africa (Nubia sub-plate) (Dewey et al., 1989; Srivastava et al., 1990; Rosenbaum et al., 2002). The trace of the plate boundary is diffuse in the Gulf of Cadiz, yet the present-day oblique WNW-ESE convergence at ~ 4 mm/yr (Koulali et al., 2011) is inferred to be accommodated by a series of 'South West Iberian Margin (SWIM)' strike-slip faults (Figure 1; Terrinha et al., 2009; Zitellini et al., 2009). Besides, the westward propagation of the Mediterranean Alpine collision belt into the Atlantic Ocean led to the emplacement of an accretionary wedge (Figure 1) during the late Miocene, referred to as the 'allochthonous unit of the Gulf of Cadiz' (AUGC) or 'olistostrome unit' (Maldonado et al., 1999; Gutscher et al., 2002; Medialdea et al., 2004; Duarte et al., 2013). The AUGC, together with the southern part of the Hercynian Iberian Massif to the north, constitutes the basement for a number of Neogene sedimentary basins in the Gulf of Cadiz, which developed and infilled during the late Miocene to Quaternary (Maldonado et al., 1999; Medialdea et al., 2004; Hernández-Molina et al., 2016a). As a result of the underlying unstable AUGC and the oblique convergence between the Iberia and Nubia sub-plates, sedimentation in these basins has been affected by tectonic processes such as episodic uplift of fault blocks, fault reactivation and diapirism (Maldonado et al., 1999; Gràcia et al., 2003; Medialdea et al., 2004; Fernández-Puga et al., 2007; García et al., 2009; Terrinha et al., 2009; Zitellini et al., 2009; Duarte et al., 2011).

2.2. Oceanographic setting

The oceanographic regime over the northern Gulf of Cadiz upper slope is controlled by the exchange of Atlantic and Mediterranean water masses through the Strait of Gibraltar (e.g. Price et al., 1993). This exchange started after the opening of the Strait of Gibraltar in the latest Miocene (Duggen et al., 2003; Roveri et al., 2014), increased during the Pliocene, and eventually reached the present-day intensity during the Quaternary (e.g. Hernández-Molina et al., 2014b).

Atlantic waters flowing eastward towards the Mediterranean are related to the Azores Current, which is part of the large-scale Subtropical Gyre dominating the (sub)surface circulation in the low- to mid-latitude North Atlantic (McIntyre et al., 1976; Schmitz and McCartney, 1993; Bahr et al., 2018). In the Gulf of Cadiz, they comprise a shallow water mass, from 0 – ~100 m water depth (referred to as North Atlantic Superficial Water - NASW; Hernández-Molina et al., 2016a), and the Eastern North Atlantic Central Water (ENACW), between ~100 – 300 m water depth (Bellanco and Sánchez-Leal, 2016). The NASW bounds landwards two cyclonic shallow-water circulation cells that occupy the continental shelf off SW Iberia and which are controlled by the prevailing winds (Figure 1; García-Lafuente et al., 2006a). In the study area, the eastern cell off the Guadiana River is characterized by a relatively high reworking activity of waves and alongshore currents (Lobo et al., 2004). The ENACW affects the outer shelf and part of the upper continental slope (Figure 1) and is characterized by an average temperature of ~14.5 °C and relatively low salinity (< 36.2) and velocity (< 0.2 m/s), with intra-annual changes caused by variations of the water column stratification (Bellanco and Sánchez-Leal, 2016; Sánchez-Leal et al., 2017). The longer-term (i.e. on kyr to Myr timescales) variability in the physical properties and flow depth of the ENACW in the Gulf of Cadiz is more elusive, yet this is suggested to be influenced by changes in the interaction with the underlying Mediterranean Outflow Water (see below; Nelson et al., 1999; Jia, 2000; Volkov and Fu, 2010; Bahr et al., 2018; Roque et al., 2019), and by large-scale changes in atmospheric wind fields in the North Atlantic region. The latter changes are connected to shifts in the position of the polar front, and drive fluctuations in the strength and spatial configuration of the (sub)surface circulation systems in the low- to mid-latitude North Atlantic (McIntyre et al., 1976; Schmitz and McCartney, 1993; Bahr et al., 2018).

Underneath the ENACW, the Mediterranean Outflow Water (MOW) flows northwestward as an intermediate contour-current, at water depths down to ~1400 m (Baringer and Price, 1999; Gasser et al., 2017; Sánchez-Leal et al., 2017; Roque et al., 2019). As a result of the interaction with the seabed topography and potentially density stratification west of the Strait of Gibraltar, the MOW splits into several cores; traditionally, the Mediterranean Upper Core (MU), flowing at depths of ~300 – 800 m,

and the Mediterranean Lower Core (ML), at water depths between ~800 and 1400 m have been differentiated (Figure 1; Ambarand Howe, 1979; Borenäs et al., 2002; Millot, 2009; Copard et al., 2011; Gasser et al., 2017; Sánchez-Leal et al., 2017). Recent studies establish a more complex structure of the MOW which can comprise up to five different branches (M1 to M5 from deep to shallower), with the most surficial branch (M5) being equivalent to the MU (Sánchez-Leal et al., 2017). The MU constitutes the most relevant water mass in the upper-to-middle slope transition, flowing at a velocity of 0.4 – 0.5 m/s and average water depth of 400 m (Marchès et al., 2007). With temperatures in the range of 12.5 – 14 °C and salinity values of 36.5 – 37.5, it is less dense than the ML (Ambaret et al., 1999; Sánchez-Leal et al., 2017). The MU undergoes a significant dilution process along the upper slope of the northern margin of the Gulf of Cadiz, particularly evident west of 6°25' W, due to mixing processes with water masses of Atlantic origin (Sánchez-Leal et al., 2017). The properties of the MU also vary throughout the year, due to fluctuations in the interface depth and to mixing processes between the MOW and ENACW west of the Strait of Gibraltar (Ambaret et al., 1999; Bellanco and Sánchez-Leal, 2016; Roque et al., 2019). On longer (i.e. glacial – interglacial and stadial – interstadial) timescales, the MOW has been inferred to increase in density and hence shift to greater depths during cold intervals, leading to an enhanced ML and reduced MU during such cold (sea-level lowstand) intervals, and oppositely to a reduced ML and enhanced MU during warm (sea-level highstand) periods (Cacho et al., 2000; Llave et al., 2006; Voelker et al., 2006; Rogerson et al., 2010; Hernández-Molina et al., 2014a; Lofi et al., 2016). In a similar depth range as the MOW (~600 – 1500 m), the modified AntArctic Intermediate Water (AAIW; Figure 1), characterized by an average temperature and salinity of respectively ~10 °C and ~35.6, circulates cyclonically and seasonally pushes the MOW towards the upper continental slope (Louarn and Morin, 2011; Roque et al., 2019).

Besides the direct influence of above described water masses, other related oceanographic processes have also been shown to play a significant role along the Iberian continental margin (Hernández-Molina et al., 2016c). Amongst them, phenomena occurring in shallow to intermediate water depths in the Gulf of Cadiz include eddies, which detach from the MOW at margin promontories, submarine

canyons or banks (e.g. Serra and Ambar, 2002; Ambar et al., 2008; Pinheiro et al., 2010), and internal tides, waves and solitons, which are due to disturbances at the density interface between water masses. These interface phenomena are especially well documented in and around the Strait of Gibraltar (e.g. Richez, 1994; Brandt et al., 1996; Izquierdo et al., 2001; Bruno et al., 2002; Vlasenko et al., 2009; Sánchez-Garrido et al., 2011), but have been reported at various upperslope to shelfmargin sectors along the SW Iberian margin as well (e.g. Apel, 2004; Bruno et al., 2006; da Silva et al., 2007; Quaresma and Pichon, 2013).

2.3. Sediment supply

Sediment supply to the northern Gulf of Cadiz shelf and upperslope is dominated by the fluvial input from the Guadiana and Guadalquivir rivers (Figure 1A), which drain most of the southern half of the Iberian Peninsula (Lobo et al., 2018). Their mean water discharges have been estimated at 80 m³/s and 160 m³/s respectively (van Geen et al., 1997). Suspended sediments deriving from these rivers disperse towards the east to south-east because of the NASW circulation pattern over the shelf (Gutierrez-Mas et al., 1996; Nelson et al., 1999). Minor sediment contributions come from smaller rivers such as the Piedras and Tinto-Odiel. There is a reduction in fluvial sources west of the Guadiana River, making the southern Portuguese (Algarve) shelf a sediment-starved area (Lobo et al., 2004).

2.4. Upper continental slope physiography, geomorphology and stratigraphic architecture

The SW Iberian continental margin can be laterally subdivided into a western sector marked by the occurrence of submarine canyons (off S to SW Portugal), a central, smooth, strongly progradational sector without submarine canyons (off the Guadiana and Guadalquivir rivers), and an irregular eastern sector (close to the Strait of Gibraltar) with slope incisions (Hernández-Molina et al., 2006; Mulder et al., 2009).

In the central sector, which is of interest for this study, the shelf margin is located at water depths ranging between 110 and 150 m (Nelson et al., 1999; Maldonado et al., 2003). Overall, it exhibits a smooth and prograding morphology (Llave et al., 2001), mainly covered by coarse-grained (sandy and

gravelly) sediments (Nelson et al., 1999). The continental slope can be subdivided into three subdomains (upper, middle and lower) according to the slope profile and large-scale morphology. The upper slope (~130 – 450 m water depth) is particularly relevant for the purpose of this study and is characterized by a width of 10 – 20 km and slope gradients between 1 and 3° (Hernández-Molina et al., 2006). The regional morphology of the upper slope is relatively homogeneous, as it represents the surficial expression of a clinoform pattern along most of the margin. This configuration is interrupted west of the Guadiana River, where a well-marked erosional surface establishes the boundary with the Alvarez Cabral contourite moat, that extends for about 80 km and is 4 – 11 km wide (Hernández-Molina et al., 2003; García et al., 2009). Detailed morphological observations on the upper slope are mostly limited to the area next to the Strait of Gibraltar, and include pockmarks (Baraza and Ercilla, 1996; Casas et al., 2003), downslope-oriented gullies (Nelson et al., 1999; Hernández-Molina et al., 2014a) and scarps and slumps (Baraza et al., 1999; Hernández-Molina et al., 2006), of which one particular example has later been suggested to represent a sediment wave field instead (Lee et al., 2002).

The late Quaternary stratigraphic architecture of the upper slope is dominated by the progradational stacking of shelf-margin wedges, which formed in response to successive ~100 kyr (i.e. eccentricity-driven) glacio-eustatic cycles (Lobo et al., 2005). These sediment wedges are bounded by subaerial unconformities on the shelf that formed during glacial lowstand intervals. For example, the upper boundary of the most recent widespread shelf-margin wedges is a regional erosional surface attributed to the prolonged sea-level fall leading into the Last Glacial Maximum (LGM) (Lobo et al., 2018; Mestdagh et al., 2019). Tectonics modulate the late Quaternary stacking pattern of these major seismic units as marked by the occurrence of two distinct progradational/uplift phases, whereas oceanographic processes impact on their depocenter distribution (Mestdagh et al., 2019). As on many other modern continental margins, the shelf-margin wedges are internally dominantly composed of (deltaic) regressive facies deposited during gradual sea-level falls and occasionally lowstand intervals; on the other hand, transgressive (to highstand) deposition is generally thin or absent (Lobo and Ridente, 2014; Mestdagh et al., 2019). The post-LGM deglaciation is the best resolved transgressive

phase in the upper slope seismic record and features a 35 km long plastered drift in the upper-to-middle slope transition off the Guadiana River, which further attests of the influence of (alongslope) oceanographic processes on the upperslope (Llave et al., 2007; Mestdagh et al., 2019).

3. Material and methods

3.1. Seismic data

3.1.1. Acquisition, processing and interpretation

The high-resolution reflection seismic profiles used in this study (Figure 1B) were collected during the RV Belgica COMIC and RV Ramón Margalef LASEA cruises, both in 2013. These surveys deployed a single-channel streamer and SIG sparker source with an energy of 300 J, a shot interval of 2 s and a sampling frequency of 10 kHz. The achieved vertical resolution was $\sim 1 - 1.5$ m. The processing procedure included bandpass filtering (Ormsby type), amplitude correction (spherical divergence), 2D spike (burst noise) removal, swell static corrections and top muting. This data was complemented with LASEA 2013 parametric echosounder (TOPAS) profiles, and with reflection seismic profiles collected during previous surveys in the study area such as the GOLCA93, FADO 1996 and WADIANA 2000 campaigns, which used 3.5 kHz sub-bottom profilers and uniboom systems (Geopulse) as seismic sources (Figure 1B).

The analysis focuses on the characterization of morphological and stratigraphic features on the shelf margin and upper slope which stand out from the background seismic facies (i.e. a parallel-oblique progradational reflection configuration; Lobo et al., 2005; Mestdagh et al., 2019). Seismic profiles are selected to illustrate the variability in morphological and stratigraphic classes along the study area. The identified classes are subdivided into four main genetic categories (depositional, erosional, mixed depositional-erosional and 'other'). Specifically, their primary characteristics, including seismic facies, shape and orientation, their location on the slope, and their stratigraphic position, are described. Where morphometric information on the analyzed features is converted from two-way travel time (twtt, in seconds) to metric dimensions, a p-wave velocity (V_p) in the (shallow) subsurface of 1600 m/s was adopted, which is an average value derived from core and downhole logging measurements in the upper ~ 100 m of boreholes at IODP sites U1386/U1387 (Stow et al., 2013; Mestdagh et al., 2019).

3.1.2. Seismicstratigraphicframework

Stratigraphicunits and surfaces are indicated in those seismicprofiles that could be correlated to the seismic stratigraphic framework of Mestdagh et al. (2019). This framework is dated through the borehole-seismic tie at IODP Expedition 339 sites U1386 and U1387 on the middle continental slope (Figure 1B; Stow et al., 2013; Mestdagh et al., 2019), and correlates the middle slopeto the continental shelf record; as such, it also encompasses the upperslopesectorinvestigated in this study. Five major late Quaternary seismic units (U1 to U5, from youngest to oldest) have been delineated, which correspond to the five most recent ~100 kyr glacio-eustaticcycles from marine isotope stage (MIS) 12 till present; these units are bounded by margin-wide surfaces mws1 to mws5 (Table 1; Mestdagh et al., 2019). Internally, the basal sub-units (U1, U2.2, U3.4, U4.2 and U5.2) are formed under transgressive to highstand conditions (Table 1; hereinafter referred to as ‘transgressive’ intervals), whereas the upper sub-units (U2.1, U3.1, U4.1 and U5.1) are formed under regressive to lowstand conditions (Table 1; hereinafterreferredto as ‘regressive’ intervals). U3 comprises two additionalsub-units (U3.3 and U3.2) between the basal and upper sub-unit, which respectively formed under the stadial sea-level fall into MIS7d and subsequent interstadialsea-levelriseinto MIS7csuperimposed on the 100 kyr glacio-eustaticcyclicity (Table1; Mestdagh et al., 2019).

3.2. Bathymetricdata

Low-resolution bathymetricdata(with a 115 x 115 m grid resolution) covering the entire continental margin were obtained through the EMODnet online portal (EMODnet Bathymetry Consortium, 2018). High-resolution multibeam datawere collated from three oceanographicexpeditions by the Instituto Español de Oceanografía (IEO) that were part of research projects LIFE+ INDEMARES/CHICA (2011), ARSA (2013) and ISUNEPCA (2014). These data were acquired with Kongsberg Simrad EM-300 (operating at a frequency of 30 kHz and emitting 135 soundings per swath) and EM-710 (70-100 kHz and 400 soundings per swath) multibeam echosounder systems (MBES), operating in high-density mode and using pitch and yaw stabilization. The CARIS HIPS & SIPS 9.0 data processing software was

used to produce a 15 × 15 m bathymetric grid model covering an area of 600 km² between ~100 and 500 m water depth.

3.3. Oceanographic data

Salinity data were retrieved from the World Ocean Database (WOD) 2018 (Boyer et al., 2018) and visualized using Ocean Data View (Schlitzer, 2017). Salinity values were plotted in two longer cross-sections over the upper slope (one in the eastern and one in the western part of the study area, indicated in purple in Figure 1B) and over two of the available seismic profiles, to identify the various water masses and illustrate their present-day distribution. These salinity plots are generated by interpolating data from adjacent CTD stations acquired during similar periods of the year (winter season in this case, to avoid mixing signals in case of seasonal variations).

In order to estimate the interaction of internal waves with the upper slope topography, ratios of the slope angle (γ) over the internal wave/tide energy propagation angle relative to the horizontal (c) were estimated along one single upper slope transect. The parameter c is given by the following formula (Cacchione et al., 2002):

$$c = \left(\frac{(\sigma^2 - f^2)}{(N^2 - \sigma^2)} \right)^{1/2}$$

where σ is the internal wave frequency (in cycles per hour; cph), N is the Brunt-Väisälä or buoyancy frequency (in cph), and f is the local inertial frequency or Coriolis parameter (in cph), which depends on the latitude ϕ according to the formula $f = (\sin \phi)/12$. In the absence of direct measurements, a theoretical value of $\sigma = 0.081$ cph is adopted assuming the dominance of semi-diurnal M2 internal tides (Cacchione et al., 2002), which have been reported to propagate at shallow and intermediate water depths around the Iberian margin (Azevedo et al., 2006; García-Lafuente et al., 2006b; Pichon et al., 2013). The variation of N with depth was calculated using Ocean Data View, based on 10 CTD stations (from WOD18) along the section and applying a moving average filter to reduce noise. When $\gamma/c \approx 1$ (so-called 'critical' conditions), internal wave/tide energy is trapped along the seabed and

current velocities intensify, whereas undersubcritical ($\gamma/c < 1$) or supercritical conditions ($\gamma/c > 1$) the internal wave or tide characteristics get respectively reflected upslope (transmitted) or reflected downslope (Cacchione and Wunsch, 1974; Cacchione et al., 2002; Lamb, 2014; Ribó et al., 2016).

4. Results

4.1. Morphological characterization of the upper-slope sea floor

Detailed multibeam bathymetric data of the study area reveal the occurrence of a number of morphological features at the present-day seafloor (Figure 2A).

In the east, between 270 and 400 m water depth, a linear to slightly curved depression with a NW-SE orientation can be observed (Figure 2B). It is ~11 km long, 1 km wide and 2 m deep. In the NW this feature becomes less marked and is associated with a number of (semi-)circular depressions with an average diameter and depth of 60 and 1.3 m respectively. At its SE end, a positive semicircular irregular relief that is ~5 m high and 450 m in diameter occurs within the elongated depression (Figure 2B).

A field of undulations covering ~20 km² can be observed on the central lower part of the study area between 400 and 440 m water depth (Figure 2C). The crests of these undulations are linear to slightly sinuous, have lengths between 1.5 and 5 km, and are oriented parallel to the trend of the continental slope (Figure 2C). The spacing between the crests is 400 m on average, while their amplitudes (i.e. crest-to-trough heights) are around 1.5 m.

A N-S elongated positive relief, with a length of ~3 km, width of ~700 m and height of up to 2 m, can be observed NW of the undulation field (Figure 2D), between 350 and 430 m water depth. The western edge of this feature is flanked by a downslope-running depression with a width and depth of 150 and 1 m respectively. The positive relief exhibits abundant (around 40) superimposed (semi-)circular depressions with diameters up to 100 m and depths up to 2 m (Figure 2D).

In the western part of the study area (between 170 and 210 m water depth), a linear, along-slope-running break-of-slope can be observed below the shelf margin (Figure 2E). This feature is characterized by relatively steep slopes (4 – 7°) compared to the rather flat shelf and more gently dipping upper slope. Several semicircular depressions with depths of 1 – 2 m and diameters of 70 – 140 m are also observed in this location, scattered over the shelf margin (Figure 2E).

Another seabed crenulation zone can be observed towards the western lower part of the upper slope between 420 and 450 m water depth (Figure 2F). This feature consists of a series of short (max. 1.5 km), sinuous slope-parallel undulations (~2 m high), an elliptic depression of 4 m deep and 700 m long, and a few smaller semicircular depressions to the N, with depths around 2 m and diameters up to 150 m (Figure 2F).

4.2. Characterization and classification of morphological features in seismic reflection data

A range of morphological features can be identified in the seismic profiles crossing the upper slope and shelf margin in the study area. These features are characterized and classified in the below section (summarized in Table 2). The various classes are denoted in the seismic profiles shown in Figures 3 – 11 using the symbols in Table 2.

4.2.1. Depositional features

Seven morphological classes have been typified as depositional features. Morphological class 1 is characterized by low-amplitude, (sub)parallel continuous reflections, generally dipping seaward at low angles (0.5 – 1.5°) and organized in sheeted to wedge-shaped sediment bodies (Table 2). This class can be observed on the middle to lower part of the upper slope, dominantly composing the older transgressive sub-units in the eastern part of the study area (Figures 3 – 7).

The seismic facies of class 2 features (sub)parallel and generally seaward dipping (0.5 – 4°) continuous reflections of moderate to high amplitude. This class occurs over the entire upper slope in sheeted to wedge-shaped bodies (Figures 5 – 7) or locally as an infill of underlying depressions (Figures 4 and 9), dominantly within the regressive sub-units.

Continuous (sub)parallel reflections of moderate-high amplitude constitute the seismic facies of morphological class 3 as well. They can be observed on the upper to middle part of the upper slope, onlapping the basal bounding surface of U1 (Figures 3 and 4) and, significantly, showing a subtle mounded geometry towards the west (Figure 10).

Class 4 is composed of wavy, continuous, moderate- to high-amplitude reflections that form asymmetric undulations. The upslope flank of these undulations is generally thicker, shorter and less steep than the downslope flank, which makes that the crests show an upslope migration through time (Figures 3 and 5). They can be observed on the lower part of the upper slope within U1, with wavelengths and heights of 400 – 600 and 1.5 – 5 m respectively (Figures 3 and 5).

Wavy, continuous reflections of variable amplitude also characterize the seismic facies of morphological class 5. The resulting undulations are more symmetric and show less pronounced upward migration trends than class 4 (described above), with varying dimensions (wavelengths in the range of 300 – 900 m and heights between 2 and 15 m). These undulations can be found from the upper to lower part of the upper slope in the eastern sector of the study area, dominantly within regressive sub-units (Figures 3 and 5 – 8).

Class 6 is marked by irregular or contorted discontinuous reflections with variable amplitudes, confined locally (i.e. interspersed between other depositional classes, e.g. Figures 6 and 7) or extending over larger stretches of the upper slope (e.g. Figure 8). This class can be observed on the entire upper slope, dominantly in regressive sub-units, both in the eastern and western part of the study area (Figures 3 – 10).

Chaotic, discontinuous reflections, organized in low-amplitude to transparent bodies with irregular or smooth basal surfaces and irregular high-amplitude top surfaces characterize morphological class 7. They can be observed on the lower part of the upper slope in the east of the study area within regressive sub-unit U2.1 (Figures 3 and 5).

4.2.2. Erosional features

Four morphological classes are considered as erosional features. Morphological class 8 comprises linear, v-shaped erosional features with a depth of ~3 m and width of ~80 m that have an overall downslope orientation. They can sporadically be observed within (regressive) sub-unit U2.1 in the eastern part of the study area (Figure 7).

Class 9 is also characterized by linear erosional depressions, but with an overall along-slope orientation. These features, with a depth and width of ~3 and ~150 m respectively, can be observed on the uppermost part of the upper slope within transgressive unit U1, both in the eastern and western part of the study area (Figures 4, 9 and 10). Successive furrows within U1 show an upslope migration through time.

Irregular, large-scale erosional surfaces which truncate and locally deeply incise (up to 0.06 s twtt or ~50 m) underlying strata, constitute morphological class 10. They can be observed on the shelf margin at the base of U1 (Figure 11), and on the upper to middle part of the eastern upper slope (Figures 4 and 9). In the latter case, they define an overall downslope-oriented erosional system within regressive sub-unit U2.1. These surfaces laterally correlate to more planar erosional or conformable surfaces.

Class 11 features along-slope-oriented, elongated, planar and regular erosional surfaces on the outer shelf and upper part of the upper slope. They occur at the base and top of transgressive unit U1, and are most pronounced in the western part of the study area (Figures 4 and 10).

4.2.3. Mixed depositional and erosional features

One morphological category (class 12) is considered as mixed, and is characterized by an along-slope-running seafloor break-of-slope below the shelf break in the western part of the study area (Figure 10). It is marked by sloping angles of 1 – 2°, interspersed between gradients of 2.5 – 3.5° downslope and 6 – 8° upslope. This feature occurs on top of erosional classes 9 and 11, and bounds the upslope end of depositional class 3 (Figure 10).

4.2.4. Other features

Finally, two morphological classes cannot be categorized as depositional, erosional or mixed. Class 13 typifies a low-amplitude transparent columnar body with chaotic reflections. It can be observed on the central part of the upper slope towards the east of the study area (Figure 6), where it pierces U5 to U2 (and underlying strata). In 2D it is 1.5 km wide and at least 0.35 s twtt high.

Morphological class 14 comprises isolated, (very) high-amplitude spots, which occur randomly from the upper to lower part of the upper slope in the eastern sector of the study area (Figures 3A - 8A). They can also be clustered at specific seismic horizons (e.g. at the top of sub-unit U3.2; Figures 3A – 8A), or within the crests of the wavy reflections of class 5 (Figure 3).

4.3. Hydrographic results

All salinity plots (Figures 12A to 12D) display a highly saline water mass (salinity > 36.5) draping the middle slope and the lower part of the upper slope, which corresponds to the upper core of the MOW (Ambaret et al., 1999; Sánchez-Leal et al., 2017). It underlies a less saline water mass (salinity < 36.2) and surficial waters (with a salinity range of 36.2 – 36.5), which accord with the characteristics of the ENACW and NASW respectively (Bellanco and Sánchez-Leal, 2016; Hernández-Molina et al., 2016a; Sánchez-Leal et al., 2017). The salinity contrast between the MOW and ENACW/NASW is higher in the east than in the west of the study area (Figure 12A vs. 12B). Consequently, the interface between the MOW and ENACW is rather sharp and intersects the seafloor at ~320 m water depth in the east (Figure 12A), whereas it is more diffuse in the west (affecting the upper slope seabed between ~300 – 400 m; Figure 12B). The ENACW and NASW also have a rather gradual interface between ~100 – 200 m water depth in the open ocean (Figures 12A – 12C). Closer to the shore, a smaller water mass core (~60 m high and ~3 km wide) characterized by salinities between 36.2 and 36.4 can be observed running along the upper slope at water depths of 210 – 260 m in the east and 150 – 210 m in the west (Figures 12A and 12B).

The calculated γ/c values over the upper slope shown in Figure 12D demonstrate that the reflection conditions for internal waves at the seafloor are critical (i.e. $\gamma/c \approx 1$) from 250-300 and 340-430 m water depth. Between these two zones with critical slopes, the reflection conditions are supercritical ($\gamma/c > 1$; between 300 and 340 m), whereas the reflection conditions are subcritical ($\gamma/c < 1$) further downslope towards the middle slope and upslope towards the shelf (Figure 12D).

5. Discussion

5.1. Interpretation and origin of upperslope morphological features

The morphological features identified in the bathymetric and reflection seismic data are interpreted in this section, along with a discussion of their origin and dominant controlling processes (summarized in Table 3). Their spatial distribution is mapped in Figure 13, with a distinction between transgressive to highstand (interglacial) intervals (Figure 13A) and regressive to lowstand (glacial) intervals (Figure 13B).

5.1.1. Background sedimentation

The stratified (parallel-continuous) facies of morphological classes 1 and 2 (Table 2), which are further devoid of distinct morphological features, are prevalent and constitute the background sedimentation on the studied upperslope sector. Based on their combined external geometry, classes 1 and 2 can be labelled as shelf-margin wedges (in line with Lobo et al., 2005; Mestdagh et al., 2019). With respect to the sedimentary environment, the lower-amplitude seismic facies of class 1 is inferred to be indicative of fine-grained sedimentation and the dominance of hemipelagic sedimentation, and is therefore interpreted to represent a 'hemipelagic wedge' depositional environment (following Prather et al., 2017). On the other hand, class 2 shows higher-amplitude facies suggesting the input of coarser-grained (terrigenous) sediments as well (e.g. Chiocci, 2000), which likely happens through enhanced deposition from (downslope) sediment gravity flows (e.g. turbidity currents). Hence, this class can be interpreted to represent a 'shelf-margin delta' setting (following e.g. Morton and Suter, 1996; Porębski and Steel, 2003; Pratson et al., 2007; Steel et al., 2008).

5.1.2. Plastered drift and associated alongslope-controlled features

Within the youngest seismic unit U1, several morphological features modulate the above described uniform background pattern of classes 1 and 2. The largest-scale depositional feature is the slightly mounded and alongslope elongated body with subparallel overlapping reflections of morphological class 3 (Table 2; Figures 4 and 10), which is interpreted as a plastered drift. This interpretation is based on

the criteria for identifying contourite drifts of McCave and Tucholke (1986) and Faugères et al. (1999), and follows earlier work by Llave et al. (2007) and Mestdagh et al. (2019). At the upper boundary of the plastered drift, the occurrence of alongslope-oriented erosional elements further attests of the present-day activity of bottom currents in this part of the study area (Figure 13A): (i) a series of stacked linear depressions (class 9; Figures 4 and 10), interpreted as (buried) upslope migrating small-scale contourite moats (following García et al., 2009), and (ii) an alongslope elongated erosion surface (i.e. class 11) at the present-day seabed in the western part of the study area (Figures 2E and 9), which is commonly observed in upper slope settings adjacent to contourite drifts (Faugères et al., 1999; Hernández-Molina et al., 2008). This steep erosional surface, together with the relatively flat depositional upper part of the plastered drift, forms a step in the slope profile below the shelf break (Figure 10; described as morphological class 12). This break-of-slope can thus be interpreted as a (contourite) terrace, in analogy with examples reported along the SW Atlantic margin (Hernández-Molina et al., 2009; Preu et al., 2013; Hernández-Molina et al., 2016b) and NW Mediterranean Sea (Miramontes et al., 2019).

Assuming that the plastered drift in the western seismic profiles (Figure 10) connects to the (more subdued; see discussion section 5.2.1) plastered drift in the eastern profiles (Figures 3 – 4), it has a length (in alongslope direction) of at least 40 km, and is located between ~170 and 430 m water depth (Figure 13A). Plastered drifts generally develop in settings with low slope gradients (Faugères et al., 1999) where weak bottom currents are interspersed between zones of more intense bottom-current flow up- and downslope (Rebesco et al., 2014; Miramontes et al., 2019). In the study area, the vigorous water mass bounding the upper end of the plastered drift is the ENACW, which at present flows along the upslope and outer shelf between 100 and 300 m water depth (Figures 12A-D). This water mass is focused in an overall eastward-flowing baroclinic jet known as the Gulf of Cadiz Current (GCC; Figure 12C), which shows a persistent, meandering behavior with average velocities around 0.1 – 0.15 m/s and maxima up to 0.3 – 0.4 m/s (García-Lafuente et al., 2006a; Peliz et al., 2007; Peliz et al., 2009; Bellanco and Sánchez-Leal, 2016). A small core that is likely related to the GCC occupies the above

discussed contour terrace (Figure 12C), and is thus interpreted to be responsible for the along-slope-oriented erosional surface (in the western part of the study area) and small-scale moats at the upper boundary of the plastered drift. The vigorous water mass flowing over the central to lower part of the plastered drift is the upper core of the MOW (Figure 12A-D), which on the middle slope to the S and SW also shapes the sheeted Faro-Cadiz and Bartolome Dias drifts, the mounded Faro-Albufeira drift and the Alvarez-Cabral moat of the CDS (Hernández-Molina et al., 2006; Llave et al., 2007; García et al., 2009).

This plastered drift developed throughout U1, which encompasses the last deglaciation (following the LGM) and Holocene highstand (see stratigraphic framework in Table 1; Mestdagh et al., 2019). The fact that the upper MOW at present flows over the central part of the drift (Figure 12C) and not deeper, bounding its distal end (as is normally observed for actively growing plastered drifts; Hernández-Molina et al., 2008; Miramontes et al., 2019), might indicate that the drift has dominantly developed during the early phase of the post-LGM transgression. At that moment, the ENACW started to strengthen and still occupied the entire upper slope, while the upper MOW was confined to greater depths (i.e. a situation under which the observed position of the plastered drift conforms to the generally accepted models; Hernández-Molina et al., 2008; Miramontes et al., 2019). Later, as the upper core of the MOW shallowed and started to occupy the lower/central part of the upper slope during the Holocene highstand (until present), the established drift morphology was maintained without significant drift construction. The latter is likely linked to the severe reduction in sediment supply to the upper slope under high sea-level positions (as further discussed in section 5.2).

5.1.3. Sediment waves

On a smaller scale, two types of undulations have been identified in the seismic record of the study area (classes 4 and 5; Table 2). The undulating bedforms described in morphological class 4 occur within U1, superimposed on the lower part of the above described plastered drift (Figures 3 and 5). The expression of these features at the seabed can furthermore be tied to the field of seabed

undulations appearing in the multibeam data (Figure 2C). Given their asymmetric geometry, upslope migration pattern (thicker upslope flanks vs. thinner downslope flanks) and similarity in dimensions and internal structure between adjacent waves, they are interpreted as depositional sediment waves (as opposed to post-depositional deformational features), following earlier interpretations in the northern Gulf of Cadiz by Lee et al. (2002) and the criteria outlined in Wynn and Stow (2002) and Urgeles et al. (2011). The slope-parallel orientation of the wave crests (Figure 2C) suggests that the genesis of these sediment waves is linked to across-slope currents over the sea bottom (Wynn and Stow, 2002; McCave, 2017).

A first possible mechanism for generating such across-slope currents and associated sediment waves is the breaking of internal waves or tides against the continental slope (e.g. King et al., 2014; Belde et al., 2015; Delivet et al., 2016; Droghei et al., 2016; Ribó et al., 2016; van Haren and Puig, 2017; Collart et al., 2018; Reiche et al., 2018; Yin et al., 2019). The position of the sediment wave field on the modern seabed, at the boundary between the upper MOW and ENACW (Figure 12D) supports this interpretation, as internal waves typically propagate along the interface between water layers of different densities (Shanmugam, 2013). Furthermore, calculations for the modern oceanography over northern Gulf of Cadiz continental slope indicate that critical internal wave reflection conditions prevail over the sediment wave field ($\gamma/c \approx 1$; Figure 12D). Internal wave or tide energy, if any, would thus be trapped along the seabed and intensify current velocities, optimizing the conditions for the development of sediment waves (Cacchione and Wunsch, 1974; Cacchione et al., 2002; Lamb, 2014; Ribó et al., 2016). Internal waves have previously been documented in the Gulf of Cadiz, mainly occurring as solitary waves or 'solitons' affecting the upper tens to hundreds of meter of the ocean west of the Strait of Gibraltar (Apel, 2004; Hernández-Molina et al., 2016c), and internal tides have been suggested at the ENACW-MOW interface at the Ferrol canyon on the NW Iberian margin (Collart et al., 2018). Yet, future oceanographic measurements (e.g. long-term moorings) are needed to unequivocally confirm the activity of internal waves or tides at the ENACW-MOW boundary at the specific location of the here presented modern sediment wave field.

Alternatively, across-slope currents over sediment wave fields can be related to downslope turbidity currents (e.g. Normark et al., 1980; Wynn et al., 2000; Migeon et al., 2001; Ercilla et al., 2002; Gonthier et al., 2002; Lee et al., 2002; Lonergan et al., 2013; Normandeau et al., 2019), which could occur at the present-day seabed in the northern Gulf of Cadiz as well (albeit in an unconfined fashion, since major submarine channels or canyons to focus confined flows are absent at the present-day seafloor; Figure 2). Theoretical work by McCave (2017) has shown that sediment waves can form (as antidunes) under turbidity currents when the slope gradient exceeds 0.3 % (i.e. $\sim 0.2^\circ$; this condition is fulfilled on the entire upslope; Figure 12E), with a progressive decrease in wave dimensions downslope (Lee et al., 2002; Wynn and Stow, 2002). Accordingly, if the sediment waves at the present-day seabed (Figure 2C) formed under turbidity currents, one would expect them also to occur higher up the slope with greater heights and wavelengths, and not only in the observed restricted depth interval ($\sim 400 - 440$ m) at the foot of the upslope. The role of turbidity currents in the formation of this modern sediment wave field is therefore considered to be limited. On the other hand, the (mostly buried) undulations of class 5 (Table 2), which are equally interpreted as depositional sediment waves based on their (slight) asymmetry, upslope migration and reflection continuity/similarity between adjacent waves (Lee et al., 2002; Wynn and Stow, 2002; Urgeles et al., 2011), do occupy the entire upper slope and show downslope decreasing dimensions (e.g. within U3.1 in Figure 5). Turbidity currents are consequently inferred to be the dominant factor in the formation of this class of sediment waves (Table 3).

A temporal pattern (more generally discussed in section 5.2.2) in the dominant formation mechanism of the observed sediment waves can thus be inferred: during interglacial intervals, when the upper core of the MOW circulates along the upslope (as illustrated in Figure 12), class 4 sediment waves form under the action of internal waves at the ENACW-MOW interface; during glacial intervals, this interface deepens (e.g. Llave et al., 2006; Bahr et al., 2014; Kaboth et al., 2016), and class 5 sediment waves rather develop on the upslope under the action of turbidity currents.

5.1.4. Subaqueous massmovements

Morphological classes 6 and 7 (Table 2) are interpreted to represent slumps and debrites respectively, following recent classifications and definitions for products of subaqueous mass movements (Talling et al., 2012; Shanmugam, 2018), and thus reflect the activity of downslope gravity-driven processes (Table 3). This interpretation is based on the expression of these features in the reflection seismic profiles (Figures 3 – 9), more specifically on the irregular, contorted reflection configuration for the slumps, and on the chaotic, very low amplitude seismicfacies forthe debrites. In the multibeam data, the irregular crenulation on the lower part of the slope (Figure 2F) could be a result of local gravitational mass transport processes as well, in analogywith previously reported examplesin the NE part of the Gulf of Cadiz slope (Barazaet al., 1999; Mulderet al., 2009).

5.1.5. Submarine valley system and gullies

Downslope gravity-driven processes also generate erosional elements on the northern Gulf of Cadiz upperslope. The large-scale irregular incisions in the eastern part of the upperslope (Figures 4 and 9; class 10) are interpreted to represent a submarine valley system that is bifurcated on the upperslope (Figure 13B). The more generic term ‘valley’ is adopted here instead of ‘canyon’, since the latter term implies an overall V-shaped cross-section (Shepard, 1981; Harris and Whiteway, 2011), which cannot be fully assessed herein the absence of morereflectionseismicprofiles crossing this feature. Likemost slope valley systems (Harris and Whiteway, 2011), the formation of this system is linked to submarine mass wasting events,as evidencedby its association withdebritesand the occurrence of slumpsin the sedimentary infilling of the valleys (Figures 3, 4 and 9). In addition, the upperslope valley connects to the erosional surface on the (outer) shelf at the base of U1 (Figures 4 and 9) and related incisions (Figure 11), which were previously interpreted as the subaerial unconformity and associated fluvially incised shelfvalleys developed during the last glacial period (Lobo et al., 2018; Mestdagh et al., 2019). The outer shelf valleys shown in Figure 11 occur directly landward of the upper slope valley system, suggesting that they might have been connected (as drafted in Figure 13B). This connection can also

have played an important role in the development of the slope valley system, by enhancing the delivery of sediments to the shelf break and consequent subaqueous valley incision into the slope by downslope sediment gravity flows (Shepard, 1981; Harris and Whiteway, 2011). The main erosional surface depicting the slope valleys is truncated by the basal surface of U1 (Figures 4 and 9) which formed during the LGM (Lobo et al., 2018; Mestdagh et al., 2019); hence, the initial phase of valley incision must predate the LGM and is tentatively (in the absence of precise dating) attributed to the MIS4 lowstand. This implies that this upper slope valley system was relatively short-lived since it formed, served as an (active) conduit for sediment transport to the middle slope, and eventually became inactive and infilled within a few tens of kyr; consequently, it has no expression at the present-day seabed anymore.

On a smaller-scale, few (buried) v-shaped depressions (class 8; Table 2) can be considered as (downslope) gullies (following the definition of Field et al., 1999). They occur towards the top of an upper slope section in which sediment waves of morphological class 5 are prevailing (Figure 7), and are hence inferred to have a common formation mechanism (i.e. across-slope turbidity currents). A similar genesis and association of slope gullies and sediment waves have been reported on the Gabon margin (Lonergan et al., 2013) and in the Taranaki Basin off New Zealand (Shumaker et al., 2017). In the northern Gulf of Cadiz, small-scale downslope-trending gullies occur at present on the upper slope west of the Strait of Gibraltar as well (Hernández-Molina et al., 2014a).

5.1.6. Diapirs

In line with previous work in the northern Gulf of Cadiz (e.g. Fernández-Puga et al., 2007; Llave et al., 2007; García et al., 2009; Medialdea et al., 2009; Hernández-Molina et al., 2016a), the chaotic, low-amplitude to transparent columnar body in the reflection seismic data (i.e. class 13; see Table 2 and Figure 6) is interpreted as a diapir. Diapiric structures in the Gulf of Cadiz are composed of shales, marls or salt, and are rooted in the allochthonous unit of the Gulf of Cadiz (Figure 1) or (towards the north) in underlying Triassic evaporites (Berástegui et al., 1998; Maestro et al., 2003; Medialdea et al., 2004;

Fernández-Puga et al., 2007). Some of these major known diapiric ridges border the S to SE edge of the study area (Figure 1A). Quaternary vertical movement and segmentation of these diapirs responds to pressure variations linked to (neo)tectonics (Llave et al., 2007; García et al., 2009). The here presented example (Figure 6) attests of the most recent (Late Pleistocene – Holocene) phase of diapiric activity, as it pierces sedimentary packages up to (and including) U2 (of last glacial age). The NW-SE elongated depression at the present-day sea floor in the east of the study area (Figures 2B and 6) overlies this diapir, and is likely a result of sediment collapse due to diapiric movements in the subsurface (as proposed for structures to the SE of the study area by Palomino et al., 2016). The diapir also directly affects the present-day seafloor, as the mounded circular relief (Figure 2B) is tentatively (in the absence of core material and seismic profiles crossing this feature) interpreted as a local expulsion or exhumation of diapiric material at the seafloor. Similarly, the bathymetric positive linear relief and flanking depression (Figure 2D) towards the NW could result from respectively doming and sediment collapse above another diapiric structure, a hypothesis which however needs future confirmation by reflection seismic profiling.

5.1.7. Bright spots and pockmarks

Finally, the distinct patches of enhanced reflections (class 14) are interpreted as bright spots, indicating local accumulations of free gas in the subsurface (Judd and Hovland, 1992; Løseth et al., 2009). The presence of gas on the northern Gulf of Cadiz upper slope is well documented in the east (Baraza and Ercilla, 1996; Casas et al., 2003; Fernández-Puga et al., 2007), and has been suggested to be of mixed biogenic and thermogenic origin (Díaz-del-Río et al., 2003). Interestingly, some of the bright spots are concentrated along one reflector in the crests of adjacent sediment waves (e.g. within and at the base of U3.1; Figure 3), suggesting that the wave crests can act as a trap for the gas (given that they are overlain by more impermeable sediments). In addition, the semicircular depressions at the seafloor (Figure 2), interpreted as pockmarks, indicate that some of the gas has migrated upwards and escaped at the seabed (Hovland and Judd, 1988). Currently data is lacking to verify if the pockmarks in the study

area are active at present (i.e. if gas is being released into the ocean today), yet this has been shown to be the case in the eastern sector of the Gulf of Cadiz (Baraza and Ercilla, 1996).

5.2. *Spatial and temporal patterns in the late Quaternary sedimentary evolution of the upper slope*

The mapping of the morphological classes (Figure 13) and stratigraphic control (Tables 1 and 2; Mestdagh et al., 2019) allow to evaluate the spatial distribution and temporal variation in the inferred sedimentation patterns on the northern Gulf of Cadiz upper slope.

5.2.1. Spatial patterns

Considering the entire range of identified morphological elements for both glacial and interglacial intervals, it appears that along-slope-controlled (contouritic) elements (i.e. classes 3, 9, 11, 12; Table 3) concentrate towards the western part of the study area, whereas down-slope-controlled elements (i.e. classes 2, 5, 6, 7, 8 and 10; Table 3) are more frequent towards the east (Figure 13). This spatial pattern is unlikely to be related to oceanographic conditions on the upper slope, since bottom current velocity data show (at present) no major variations in MOW/ENACW flow velocities along this margin sector (Criado-Aldeanueva et al., 2006; García-Lafuente et al., 2006a; Sánchez-Leal et al., 2017). Instead, excess sediment supply towards the eastern part of the study area is inferred to be the dominant controlling factor. Indeed, most terrigenous sediments from the major fluvial input source in the region (i.e. the Guadiana River) are dispersed south-eastwards towards the eastern sector under the influence of the cyclonic shelf circulation (Figures 1 and 13; Nelson et al., 1999; Lobo et al., 2004; García-Lafuente et al., 2006a). As a result of this contrasting sediment supply, higher sedimentation rates in the east induce more down-slope gravitational activity (e.g. Steele et al., 2008; Carvajal et al., 2009). On the other hand, along-slope products more clearly develop and preserve in the west, since they are not subdued by down-slope depositional and erosional processes (Miramontes et al., 2019).

5.2.2. Temporal variations

Superimposed on the lateral transition from a generally downslope-dominated sector in the E to an alongslope-dominated sector in the W, temporal (glacial – interglacial) variability in sedimentation style can be observed in each of these sectors (Figure 13A vs. 13B).

In the eastern sector, downslope processes and products are most prominent during glacial (regressive to lowstand) intervals (most notably U2.1) with the development of a valley system, slumps, debrites, gullies and turbidity current-controlled sediment waves (Figure 13B). Transgressive to highstand intervals (Figure 13A) are dominated by hemipelagic and deltaic background slope sedimentation, with the sporadic occurrence of internal wave-controlled sediment waves and faintly expressed contouritic elements (e.g. the moat and upper slope erosion in Figure 4). The increase in gravitational sedimentary processes during regressive to lowstand intervals is a common observation on continental margins, because more (terrigenous) sediments reach the shelf break as the shoreline migrates seawards during sea-level falls (e.g. Posamentier and Allen, 1993; Carvajal et al., 2009; Helland-Hansen and Hampson, 2009; Catuneanu, 2019). The associated increase in sedimentation rates on the upper slope also implies enhanced sediment loading, which could help precondition the slope for the inferred mass wasting events (debris flows, slumping) through underconsolidation and consequent shear strength reduction of the sediment column (e.g. Hampton et al., 1996; Laberg and Vorren, 2000; Masson et al., 2006). It is further noteworthy that regressive sub-unit U2.1 bears a stronger imprint of downslope gravitational processes than the other regressive sub-units (e.g. debrites and upper slope valleys occur exclusively within U2.1). This can be linked to a pulse of tectonic uplift during the development of U2 (inferred from seismic stacking patterns by Mestdagh et al., 2019), which further facilitated the triggering of submarine mass movements and the consequent formation of a slope valley system.

In the western part of the study area, alongslope sedimentary products (i.e. the plastered drift, moat, erosion surface and contourite terrace) are clearly manifesting within transgressive to highstand unit U1 under the influence of the oceanographic conditions established after the LGM (Figure 13A); on the

otherhand, these features are absent in the regressive to lowstand sub-units (which mainly comprise deltaic background sedimentation, occasionally affected by slumping; Figures 10 and 13B). Besides increased slope sedimentation rates during sea-level falls and lowstands (as already discussed above), the absence of bottom current-related morphological elements in the regressive to lowstand sub-units can be related to a reduction in glacial bottom current strengths in the area. The influence of the upper MOW decreases since this water mass shifts to greater depths (Llave et al., 2006; Bahr et al., 2014; Hernández-Molina et al., 2014a; Kaboth et al., 2016; Lofi et al., 2016), as does the MOW-ENACW interface. Northern Gulf of Cadiz ENACW variability over glacial-interglacial timescales is poorly constrained, yet analysis of seasonal fluctuations suggests an enhanced (GCC-related) ENACW strength after summer due to an increase in ocean stratification (Peliz et al., 2009; Bellanco and Sánchez-Leal, 2016); hence, under the premise that this mechanism can be translated to longer timescales, the ENACW would also be enhanced during interglacials and reduced during glacials. Analysis of along-slope morphological elements and associated palaeoceanographic patterns in the older transgressive/highstand intervals is impeded in this case study, because these sub-units are either not preserved (e.g. U2.2 and U4.2) on the upper slope (this is common on late Quaternary margins, Lobo and Ridente, 2014), or they are (partly) located below the multiple reflection (e.g. U3.2, U3.4 and U5.2; Figure 4).

It is finally noted that diapirs (class 13) and gas-related features (class 14) in the study area are not restricted to either glacial or interglacial intervals (Figure 13), which suggests that their governing mechanisms are not directly dependent of glacio-eustatic variations or interrelated factors.

5.3. Implications

5.3.1. Process interaction and geohazard assessment

From the above discussion, some interactions between the various morphological classes can be derived, which potentially have repercussions for geohazard assessments in the study area. Firstly, as the studied upper slope alternately records down- and along-slope products in response to glacial –

interglacial cycles (section 5.2.2; Figure 13), the effect of (contourite) drifts on slope stability should be considered. Several characteristics of plastered drifts illustrated in this work (e.g. mounded geometry, position on an inclined surface) and reported in literature (e.g. good sorting) make that they are prone to failure when loaded by sediments and/or triggered by earthquakes (Laberg and Camerlenghi, 2008). This mechanism has for example played a role in generating some of the largest known submarine slides in the world (e.g. Bryn et al., 2005; Vanneste et al., 2006), while (on a smaller scale) gravitational destabilization/remobilization of contouritic sediments has also been reported in the Gulf of Cadiz sector proximal to the Strait of Gibraltar (Mulder et al., 2003; Hernández-Molina et al., 2006). In the study area there is no direct evidence of a past link between plastered drifts and the observed mass wasting deposits (as no plastered drifts are preserved in the deeper record; see above); yet, the presence of a plastered drift at the present-day seabed is a considerable factor in assessing future slope stability, especially in combination with periodic sediment loading and seismicity.

In addition, the presence of gas in the system and diapiric activity can further promote sediment deformation and mass wasting in the study area. Free gas in the pore space reduces sediment strength (e.g. Locat and Lee, 2002; Sultan et al., 2004) and as such facilitates sliding or slumping, as already suggested in the eastern part of the Gulf of Cadiz (Baraza et al., 1999; Mulder et al., 2003). In the study area, the association of pockmarks and a possible slump at the seafloor (Figure 2F) could be a manifestation of the influence of gas on downslope gravitational processes. Deformation and sediment collapse induced by diapiric activity is also a known phenomenon in the Gulf of Cadiz (e.g. Baraza et al., 1999; Fernández-Puga et al., 2007; Hernández-Molina et al., 2016a; Palomino et al., 2016) and can be observed in the study area in the form of small-scale slumping around, and depressions above the diapir (Figures 2B and 6). Remarkably, gas-related features (bright spots, pockmarks) concentrate in the vicinity of the observed diapir (Figures 2B and 6), which can be attributed to the fact that diapir movement helps to create pathways for fluids (gas) to migrate towards the seafloor (Casas et al., 2003; Fernández-Puga et al., 2007). It should finally be noted that above potential effects of diapirism and gas can occasionally obscure the inferred temporal variation in down- and along-slope activity (section

5.2.2), as they can locally induce downslope processes and products in transgressive intervals (e.g. at the present-day seabed; Figure 2).

5.3.2. Sequence stratigraphic consideration

As a final consideration, the presented case also underlines the need for considering along-strike variability when making sequence stratigraphic interpretations of a continental margin (sector), as pointed out in recent sequence stratigraphic reviews (Catuneanu, 2006; Helland-Hansen and Hampson, 2009; Catuneanu, 2019). Sequence stratigraphic architectures are typically illustrated using 2D dip-oriented seismic sections, although laterally juxtaposed margin sectors might show significant differences in the development (i.e. timing of formation and appearance) of sequence stratigraphic surfaces and systems tracts due to differential subsidence or along-strike differences in sediment supply (e.g. Ritchie et al., 2004; Zecchin et al., 2008; Helland-Hansen and Hampson, 2009; Catuneanu, 2019). The latter mechanism is exemplified in the here presented study area, as it (despite its relatively small size of ~80 km from NW to SE) shows a partitioning between an eastern supply- and downslope-dominated sector, and a western alongslope dominated sector with reduced sediment supply (Figure 13). The increasing alongslope (bottom current) influence towards the W also implies that sequence stratigraphic interpretations for this part of the upperslope (which are beyond the scope of this work) are likely to become more complex to fit in 'standard' sequence stratigraphic models (Brackenridge et al., 2011; Mestdagh et al., 2019), whereas this might be more straightforward for the eastern sector.

6. Conclusions

This work presents the first detailed morphological analysis of the upslope and shelf margin off the Guadiana River, and as such complements earlier efforts in characterizing sedimentary processes on the northern Gulf of Cadiz upslope towards the east. The identified sedimentary products show a wide genetic diversity. Alongslope bottom currents (related to the ENACW) shape a plastered drift and associated contourite moat, terrace and erosional surface upslope. Sediment waves are attributed to either internal tides/waves at the MOW – ENACW interface or downslope turbidity currents. Downslope sediment gravity flows are responsible for the formation of a subaqueous valley system and the deposition of slumps and debrites. Finally, neotectonics and fluid (gas) flow manifest in the study area in the form of a diapiric structure, bright spots and pockmarks. These morphological classes show some interactions and distinct spatial and temporal patterns, which are caused by changes in the intensity of oceanographic processes and differential sediment supply towards the shelf edge. Specifically, the study area shows a lateral transition from a downslope-dominated margin in the E to an alongslope-dominated margin in the W, and (in terms of temporal variability) an overall increase in downslope components during glacial (regressive to lowstand) intervals. As such, this case study helps to better constrain why and predict how along- and downslope processes and their products can vary, alternate or interact on other continental margins as well.

Above findings furthermore constitute relevant input for potential future geohazard assessments and sequence stratigraphic work in the study area. In addition, they help to decipher when and how sediments are transferred from the shelf to the depositional sector of the middle slope CDS immediately downslope of the study area, which is information that so far has remained rather elusive in the assessment of the late Quaternary sedimentary evolution of this system. From a general perspective, a thorough analysis of upslope sedimentary dynamics as presented in this work thus also proves essential to better understand potential links between the stratigraphic development of shallow marine (shelf) and deeper marine (slope) settings.

Finally, by refining the seismic grid, future work in the study area should seek to delineate the extent and 3D shape of the detected features in more detail (e.g. of the subaqueous valley system, diapir, sediment wave field, plastered drift), and verify the potential presence of other (dis)similar morphological elements. As such, the identified morphological inventory could be expanded, which in turn would help to strengthen the proposed hypotheses regarding the temporal and spatial variability in upper slope sedimentation on the SW Iberian continental margin.

Acknowledgements

T. Mestdagh is funded through a doctoral scholarship of the Ghent University Special Research Fund (BOF). We would like to thank the captains, crews and scientists involved in research campaigns COMIC 2013 on board of RV Belgica and LASEA 2013 on board of RV Ramón Margalef. Ship time on RV Belgica was provided by BELSPO and RBINS-OD Nature. This research was performed in collaboration with "The Drifters" Research Group of the Royal Holloway University of London (UK), and is associated to projects CTM 2012-39599-C03, CGL2016-80445-R 'SCORE' (AEI/FEDER, UE), CTM2016-75129-C3-1-R, CGL2011-30302-C02-02 and CTM2017-88237-P. Editor Michele Rebesco and two anonymous reviewers are kindly acknowledged for providing constructive feedback.

Table captions

Table 1. Seismic stratigraphic framework adopted in this study (from Mestdagh et al., 2019), with reference to the corresponding marine isotope stages (MIS) and ages. T = sub-unit formed during transgressive to highstand intervals; R= sub-unit formed during regressive to lowstand intervals.

Table 2. Characterization of morphological classes identified in the reflection seismic data (Figures 3 – 11) of the northern Gulf of Cadiz upper slope, together with their position (i.e. lower vs. upper part of the slope; eastern vs. western part of the study area) and the stratigraphic interval(s) in which they dominantly occur (T = transgressive to highstand sub-unit; R = regressive to lowstand sub-unit). The dashed part of the green line in class 10 represents the conformable (on the slope) to planar erosive (on the shelf) lateral correlation of the incised erosional surfaces (in full green line).

Table 3. Interpretation and dominant formation mechanism(s) of the morphological classes described in Table 2.

Figure captions

Figure 1. (A) Map of the Gulf of Cadiz, indicating the pathways of the major water masses (NASW = North Atlantic Superficial Water; ENACW = Eastern North Atlantic Central Water; MOW = Mediterranean Outflow Water, MU = upper core, ML = lower core; AAIW = AntArctic Intermediate Water; NADW= North Atlantic Deep Water) and main (neo-)tectonic features (AUGC = Allochthonous Unit of the Gulf of Cadiz; PF = Portimao Fault; PH = Portimao High; CF = Cadiz Fault; SVF = S. Vicente Fault). Oceanography from García-Lafuente et al. (2006a) and Hernández-Molina et al. (2014b); tectonic features from Duarte et al. (2013); major diapiric structures from Fernández-Puga et al. (2007). **(B)** Detail of the study area on the northern Gulf of Cadiz upperslope, showing the location of the high-resolution multibeam bathymetric map of Figure 2 (white) and position of oceanographic (purple) and reflection seismic sections (red) of Figures 3 – 12. Black lines = sparker seismic profiles; grey lines = uniboom seismic profiles; dashed bluelines = TOPAS profiles.

Figure 2. (A) High-resolution multibeam bathymetric map of the study area, with the locations of the seismic profiles shown in Figures 3 – 10 (in red). **(B) –(F)** Details in grey-shaded relief of the map shown in (A), indicating the morphological features at the present-day seafloor described in section 4.1.

Figure 3. Reflection seismic profile (A) and interpretation (B) over the northern Gulf of Cadiz upper slope (location in Figure 1), with indication of the main morphological classes (legend for the identified features in Table 2). Stratigraphy from Mestdagh et al. (2019); white sub-units = transgressive, blue sub-units = regressive.

Figure 4. Reflection seismic profile (A) and interpretation (B) over the northern Gulf of Cadiz upper slope (location in Figure 1), with indication of the main morphological classes (legend for the identified features in Table 2). Stratigraphy from Mestdagh et al. (2019); white sub-units = transgressive, blue sub-units = regressive.

Figure 5. Reflection seismic profile (A) and interpretation (B) over the northern Gulf of Cadiz upper slope (location in Figure 1), with indication of the main morphological classes (legend for the identified

features in Table 2). Stratigraphy from Mestdagh et al. (2019); white sub-units = transgressive, blue sub-units = regressive.

Figure 6. Reflection seismic profile (A) and interpretation (B) over the northern Gulf of Cadiz upper slope (location in Figure 1), with indication of the main morphological classes (legend for the identified features in Table 2). Stratigraphy from Mestdagh et al. (2019); white sub-units = transgressive, blue sub-units = regressive.

Figure 7. Reflection seismic profile (A) and interpretation (B) over the northern Gulf of Cadiz upper slope (location in Figure 1), with indication of the main morphological classes (legend for the identified features in Table 2). Stratigraphy from Mestdagh et al. (2019); white sub-units = transgressive, blue sub-units = regressive.

Figure 8. Reflection seismic profile (A) and interpretation (B) over the northern Gulf of Cadiz upper slope (location in Figure 1), with indication of the main morphological classes (legend for the identified features in Table 2). Stratigraphy from Mestdagh et al. (2019); white sub-units = transgressive, blue sub-units = regressive.

Figure 9. Reflection seismic profiles over the northern Gulf of Cadiz upper slope, with indication of the main morphological classes (legend for the identified features in Table 2). Locations indicated in Figure 1. Stratigraphy from Mestdagh et al. (2019); white sub-units = transgressive, blue sub-units = regressive.

Figure 10. Reflection seismic profiles over the northern Gulf of Cadiz upper slope, with indication of the main morphological classes (legend for the identified features in Table 2). Locations indicated in Figure 1. Stratigraphic interpretation from Mestdagh et al. (2019), as far as it could be correlated to this part of the upper slope (note that this was not possible below U1 in profiles C - E); white sub-units = transgressive, blue sub-units = regressive. Data is not available for the small grey boxes in (C) and (E).

Figure 11. Reflection seismic profiles over the northern Gulf of Cadiz (outer) shelf, showing large-scale erosional incisions at the basal surface of U1 (indicated in green). Locations indicated in Figure 1.

Figure 12. (A) – (C) Present-day salinity of the water column over the northern Gulf of Cadiz upper slope in the east (A), west (B) and over the profile shown in Figure 10C (C). Locations indicated in Figure 1. Water mass annotations and interfaces follow Bellanco and Sánchez-Leal (2016): MOW = Mediterranean Outflow Water (upper branch); ENACW = Eastern North Atlantic Central Water; GCC = Gulf of Cadiz Current; NASW = North Atlantic Superficial Water. **(D)** Ratio of the slope angle (γ) over the angle of present-day internal wave energy propagation (c) along the seabed over the profiles shown in Figures 3 - 4. Critical reflection conditions (i.e. $\gamma/c \approx 1$) prevail over the lower part of the upper slope where sediment waves occur (see text for discussion). Contours indicate salinity values. **(E)** Plot of the variation of the slope angle and Brunt-Väisälä frequency (N , in cycles per hour) with depth, for the profile shown in (D). All oceanographic data retrieved from the WOD18 database (Boyer et al., 2018) and Ocean Data View (Schlitzer, 2017); red triangles indicate the positions of the CTD stations from which data was retrieved.

Figure 13. Synthesis of the spatial variation in the major sedimentary products and processes on the studied upper slope sector of the northern Gulf of Cadiz, during **(A)** interglacial (transgressive to highstand) intervals, and **(B)** glacial (regressive to lowstand) intervals. Abbreviations: IW = formed by internal waves; TC = formed by turbidity currents.

References

- Adams, E.W. and Schlager, W., 2000. Basic Types of Submarine Slope Curvature. *Journal of Sedimentary Research*, 70(4): 814-828.
- Ambar, I., Armi, L., Bower, A. and Ferreira, T., 1999. Some aspects of time variability of the Mediterranean Water off south Portugal. *Deep Sea Research Part I: Oceanographic Research Papers*, 46: 1109-1136.
- Ambar, I. and Howe, M.R., 1979. Observations of the Mediterranean Outflow-II. Deep Circulation in the Vicinity of the Gulf of Cadiz. *Deep-Sea Research Part a-Oceanographic Research Papers*, 26(5): 555-568.
- Ambar, I., Serra, N., Neves, F. and Ferreira, T., 2008. Observations of the Mediterranean Undercurrent and eddies in the Gulf of Cadiz during 2001. *Journal of Marine Systems*, 71(1-2): 195-220.
- Apel, J.R., 2004. Oceanic internal waves and solitons. In: C.R. Jackson and J.R. Apel (Editors), *Synthetic Aperture Radar Marine User's Manual*. US Department of Commerce, National Oceanic and Atmospheric Administration, pp. 189-206.
- Azevedo, A., da Silva, J.C.B. and New, A.L., 2006. On the generation and propagation of internal solitary waves in the southern Bay of Biscay. *Deep Sea Research Part I: Oceanographic Research Papers*, 53(6): 927-941.
- Bahr, A., Jiménez-Espejo, F.J., Kolasinac, N., Grunert, P., Hernández-Molina, F.J., Röhl, U., Voelker, A.H.L., Escutia, C., Stow, D.A.V., Hodell, D. and Alvarez-Zarikian, C.A., 2014. Deciphering bottom current velocity and paleoclimate signals from contourite deposits in the Gulf of Cádiz during the last 140 kyr: An inorganic geochemical approach. *Geochemistry, Geophysics, Geosystems*, 15(8): 3145-3160.
- Bahr, A., Kaboth, S., Hodell, D., Zeeden, C., Fiebig, J. and Friedrich, O., 2018. Oceanic heat pulses fueling moisture transport towards continental Europe across the mid-Pleistocene transition. *Quaternary Science Reviews*, 179: 48-58.
- Baraza, J. and Ercilla, G., 1996. Gas-charged sediments and large pockmark-like features on the Gulf of Cadiz slope (SW Spain). *Marine and Petroleum Geology*, 13(2): 253-261.
- Baraza, J., Ercilla, G. and Nelson, C.H., 1999. Potential geologic hazards on the eastern Gulf of Cadiz slope (SW Spain). *Marine Geology*, 155: 191-215.
- Baringer, M.O. and Price, J.F., 1999. A review of the physical oceanography of the Mediterranean outflow. *Marine Geology*, 155(1-2): 63-82.
- Belde, J., Back, S., Reuning, L. and Eberli, G., 2015. Three-dimensional seismic analysis of sediment waves and related geomorphological features on a carbonate shelf exposed to large amplitude internal waves, Browse Basin region, Australia. *Sedimentology*, 62(1): 87-109.
- Bellanco, M.J. and Sánchez-Leal, R.F., 2016. Spatial distribution and intra-annual variability of water masses on the Eastern Gulf of Cadiz seabed. *Continental Shelf Research*, 128: 26-35.
- Berástegui, X., Banks, C.J., Puig, C., Taberner, C., Waltham, D. and Fernández, M., 1998. Lateral diapiric emplacement of Triassic evaporites at the southern margin of the Guadalquivir Basin, Spain. *Geological Society, London, Special Publications*, 134: 49-68.
- Borenäs, K.M., Wåhlin, A., Ambar, I. and Serra, N., 2002. The Mediterranean outflow splitting - a comparison between theoretical models and CANIGO data. *Deep Sea Research II*, 49: 4195-4205.
- Boyer, T.P., Baranova, O.K., Coleman, C., Garcia, H.E., Grodsky, A., Locarnini, R.A., Mishonov, A.V., Paver, C.R., Reagan, J.R., Seidov, D., Smolyar, I.V., Weathers, K.W. and Zweng, M.M., 2018. *World Ocean Database 2018*. In: A.V. Mishonov (Editor), NOAA Atlas NESDIS 87. NOAA National Oceanic and Atmospheric Administration, Silver Spring, MD.
- Brackenkridge, R., Stow, D.A.V. and Hernandez-Molina, F.J., 2011. Contourites within a deep-water sequence stratigraphic framework. *Geo-Marine Letters*, 31(5-6): 343-360.
- Brackenkridge, R.E., Stow, D.A.V., Hernández-Molina, F.J., Jones, C., Mena, A., Alejo, I., Ducassou, E., Llave, E., Ercilla, G., Nombela, M.A., Perez-Arлуcea, M., Frances, G. and Marzo, M., 2018.

- Textural characteristics and facies of sand-rich contourite depositional systems. *Sedimentology*, 65(7):2223-2252.
- Brandt, P., Alpers, W. and Backhaus, J.O., 1996. Study of the generation and propagation of internal waves in the Strait of Gibraltar using a numerical model and synthetic aperture radar images of the European ERS 1 satellite. *Journal of Geophysical Research: Oceans*, 101(C6): 14237-14252.
- Bruno, M., Juan Alonso, J., Cózar, A., Vidal, J., Ruiz-Cañavate, A., Echevarriá, F. and Ruiz, J., 2002. The boiling-water phenomena at Camarinal Sill, the strait of Gibraltar. *Deep Sea Research Part II: Topical Studies in Oceanography*, 49(19): 4097-4113.
- Bruno, M., Vázquez, A., Gómez-Enri, J., Vargas, J.M., García Lafuente, J., Ruiz-Cañavate, A., Mariscal, L. and Vidal, J., 2006. Observations of internal waves and associated mixing phenomena in the Portimao Canyon area. *Deep Sea Research Part II: Topical Studies in Oceanography*, 53(11): 1219-1240.
- Bryn, P., Berg, K., Forsberg, C.F., Solheim, A. and Kvalstad, T.J., 2005. Explaining the Storegga Slide. *Marine and Petroleum Geology*, 22(1-2): 11-19.
- Cacchione, D.A. and Wunsch, C., 1974. Experimental study of internal waves over a slope. *Journal of Fluid Mechanics*, 66: 223-239.
- Cacchione, D.A., Pratson, L.F. and Ogston, A.S., 2002. The Shaping of Continental Slopes by Internal Tides. *Science*, 296(5568): 724-727.
- Cacho, I., Grimalt, J.O., Sierro, F.J., Shackleton, N. and Canals, M., 2000. Evidence for enhanced Mediterranean thermohaline circulation during rapid climatic coolings. *Earth and Planetary Science Letters*, 183(3-4): 417-429.
- Carvajal, C., Steel, R. and Petter, A., 2009. Sediment supply: The main driver of shelf-margin growth. *Earth-Science Reviews*, 96(4): 221-248.
- Casas, D., Ercilla, G. and Baraza, J., 2003. Acoustic evidences of gas in the continental slope sediments of the Gulf of Cadiz (E Atlantic). *Geo-Marine Letters*, 23: 300-310.
- Catuneanu, O., 2006. *Principles of Sequence Stratigraphy*. Elsevier, Amsterdam.
- Catuneanu, O., 2019. Model-independent sequence stratigraphy. *Earth-Science Reviews*, 188: 312-388.
- Chiocci, F.L., 2000. Depositional response to Quaternary fourth-order sea-level fluctuations on the Latium margin (Tyrrhenian Sea, Italy). In: D. Hunt and R.L. Gawthorpe (Editors), *Sedimentary Responses to Forced Regressions*. Geological Society, London, Special Publications, 172, pp. 271-289.
- Coleman, J.M., Prior, D.B. and Lindsay, J.F., 1983. Deltaic Influences on Shelfedge Instability Processes. In: D.J. Stanley and G.T. Moore (Editors), *The Shelfbreak: Critical Interface on Continental Margins*. SEPM Special Publication. SEPM Society for Sedimentary Geology, pp. 121-137.
- Collart, T., Verreydt, W., Hernández-Molina, F.J., Llave, E., León, R., Gómez-Ballesteros, M., Pons-Branchu, E., Stewart, H. and Van Rooij, D., 2018. Sedimentary processes and cold-water coral mini-mounds at the Ferrol canyon head, NW Iberian margin. *Progress in Oceanography*, 169: 48-65.
- Copard, K., Colin, C., Frank, N., Jeandel, C., Montero-Serrano, J.C., Reverdin, G. and Ferron, B., 2011. Nd isotopic composition of water masses and dilution of the Mediterranean outflow along the southwest European margin. *Geochemistry Geophysics Geosystems*, 12(6): Q06020.
- Criado-Aldeanueva, F., García-Lafuente, J., Vargas, J.M., Del Río, J., Vázquez, A., Reul, A. and Sánchez, A., 2006. Distribution and circulation of water masses in the Gulf of Cadiz from in situ observations. *Deep Sea Research Part II: Topical Studies in Oceanography*, 53(11-13): 1144-1160.
- da Silva, J.C.B., New, A.L. and Azevedo, A., 2007. On the role of SAR for observing "local generation" of internal solitary waves off the Iberian Peninsula. *Canadian Journal of Remote Sensing*, 33(5): 388-403.

- Delivet, S., Van Eetvelt, B., Monteys, X., Ribó, M. and Van Rooij, D., 2016. Seismic geomorphological reconstructions of Plio-Pleistocene bottom current variability at Goban Spur. *Marine Geology*, 378: 261-275.
- Dewey, J.F., Helman, M.L., Turco, E., Hutton, D.H.W. and Knott, S.D., 1989. Kinematics of the Western Mediterranean. In: M.P. Coward, D. Dietrich and R.G. Park (Editors), *Alpine Tectonics*. Geological Society, London, Special Publications, 45, London, pp. 265-283.
- Díaz-del-Río, V., Somoza, L., Martínez-Frias, J., Mata, M.P., Delgado, A., Hernández-Molina, F.J., Lunar, R., Martín-Rubi, J.A., Maestro, A., Fernández-Puga, M.C., Leon, R., Llave, E., Medialdea, T. and Vázquez, J.T., 2003. Vast fields of hydrocarbon-derived carbonate chimneys related to the accretionary wedge/olistostrome of the Gulf of Cádiz. *Marine Geology*, 195: 177-200.
- Droghei, R., Falcini, F., Casalbore, D., Martorelli, E., Masetti, R., Sannino, G., Santoleri, R. and Chiocci, F.L., 2016. The role of Internal Solitary Waves on deep-water sedimentary processes: the case of up-slope migrating sediment waves off the Messina Strait. *Scientific Reports*, 6: 36376.
- Duarte, J.C., Rosas, F.M., Terrinha, P., Gutscher, M.-A., Malavieille, J., Silva, S. and Matias, L., 2011. Thrust–wrench interference tectonics in the Gulf of Cadiz (Africa–Iberia plate boundary in the North-East Atlantic): Insights from analog models. *Marine Geology*, 289(1-4): 135-149.
- Duarte, J.C., Rosas, F.M., Terrinha, P., Schellart, W.P., Boutelier, D., Gutscher, M.-A. and Ribeiro, A., 2013. Are subduction zones invading the Atlantic? Evidence from the southwest Iberian margin. *Geology*, 41(8): 839-842.
- Duggen, S., Hoernle, K., van den Bogaard, P., Rupke, L. and Morgan, J.P., 2003. Deep roots of the Messinian salinity crisis. *Nature*, 422: 602-606.
- EMODnet Bathymetry Consortium, 2018. EMODnet Digital Bathymetry (DTM 2018). EMODnet Bathymetry Consortium.
- Ercilla, G., Alonso, B., Wynn, R.B. and Baraza, J., 2002. Turbidity current sediment waves on irregular slopes: observations from the Orinoco sediment-wave field. *Marine Geology*, 192(1-3): 171-187.
- Faugères, J.-C., Stow, D.A.V., Imbert, P. and Viana, A.R., 1999. Seismic features diagnostic of contourite drifts. *Marine Geology*, 162: 1-38.
- Fernández-Puga, M.C., Vázquez, J.T., Somoza, L., Díaz del Río, V., Medialdea, T., Mata, M.P. and León, R., 2007. Gas-related morphologies and diapirism in the Gulf of Cádiz. *Geo-Marine Letters*, 27(2-4): 213-221.
- Field, M.E., Carlson, P.R. and Hall, R.K., 1983. Seismic Facies of Shelfedge Deposits, U.S. Pacific Continental Margin. In: D.J. Stanley and G.T. Moore (Editors), *The Shelfbreak: Critical Interface on Continental Margins*. SEPM Special Publication. SEPM Society for Sedimentary Geology, pp. 299-313.
- Field, M.E., Gardner, J.V. and Prior, D.B., 1999. Geometry and significance of stacked gullies on the northern California slope. *Marine Geology*, 154(1): 271-286.
- García-Lafuente, J., Delgado, J., Criado-Aldeanueva, F., Bruno, M., del Río, J. and Miguel Vargas, J., 2006a. Water mass circulation on the continental shelf of the Gulf of Cádiz. *Deep Sea Research Part II: Topical Studies in Oceanography*, 53(11-13): 1182-1197.
- García-Lafuente, J., Díaz del Río, G. and Sánchez Berrocal, C., 2006b. Vertical structure and bottom-intensification of tidal currents off Northwestern Spain. *Journal of Marine Systems*, 62(1-2): 55-70.
- García, M., Hernández-Molina, F.J., Llave, E., Stow, D.A.V., León, R., Fernández-Puga, M.C., Díaz del Río, V. and Somoza, L., 2009. Contourite erosive features caused by the Mediterranean Outflow Water in the Gulf of Cadiz: Quaternary tectonic and oceanographic implications. *Marine Geology*, 257(1-4): 24-40.
- Gasser, M., Pelegrí, J.L., Emelianov, M., Bruno, M., Gràcia, E., Pastor, M., Peters, H., Rodríguez-Santana, Á., Salvador, J. and Sánchez-Leal, R.F., 2017. Tracking the Mediterranean outflow in the Gulf of Cadiz. *Progress in Oceanography*, 157: 47-71.

- Gonthier, E., Faugères, J.-C., Gervais, A., Ercilla, G., Alonso, B. and Baraza, J., 2002. Quaternary sedimentation and origin of the Orinoco sediment-wavefield on the Demerara continental rise (NE margin of South America). *Marine Geology*, 192: 189-214.
- Gràcia, E., Dañobeitia, J., Vergés, J., Bartolomé, R. and Córdoba, D., 2003. Crustal architecture and tectonic evolution of the Gulf of Cadiz (SW Iberian margin) at the convergence of the Eurasian and African plates. *Tectonics*, 22(4): 1033.
- Gutierrez-Mas, J.M., Hernández-Molina, F.J. and López-Aguayo, F., 1996. Holocene sedimentary dynamics on the Iberian continental shelf of the Gulf of Cádiz (SW Spain). *Continental Shelf Research*, 16(13): 1635-1653.
- Gutscher, M.A., Malod, J., Rehault, J.P., Contrucci, I., Klingelhoefer, F., Mendes-Victor, L. and Spakman, W., 2002. Evidence for Active Subduction Beneath Gibraltar. *Geology*, 30(12): 1071-1074.
- Hampton, M.A., Lee, H.J. and Locat, J., 1996. Submarine landslides. *Reviews of Geophysics*, 34(1): 33-59.
- Harris, P.T. and Whiteway, T., 2011. Global distribution of large submarine canyons: Geomorphic differences between active and passive continental margins. *Marine Geology*, 285(1-4): 69-86.
- Holland-Hansen, W. and Hampson, G.J., 2009. Trajectory analysis: concepts and applications. *Basin Research*, 21(5): 454-483.
- Hernández-Molina, F.J., Somoza, L. and Lobo, F., 2000. Seismic stratigraphy of the Gulf of Cádiz continental shelf: a model for Late Quaternary very high-resolution sequence stratigraphy and response to sea-level fall. In: D.W. Hunt and R.L. Gawthorpe (Editors), *Sedimentary responses to Forced Regressions*. Geological Society, London, Special Publications, 172, pp. 329-362.
- Hernández-Molina, F.J., Somoza, L., Vazquez, J.T., Lobo, F., Fernandez-Puga, M.C., Llave, E. and Díaz-del Río, V., 2002. Quaternary stratigraphic stacking patterns on the continental shelves of the southern Iberian Peninsula: their relationship with global climate and palaeoceanographic changes. *Quaternary International*, 92: 5-23.
- Hernández-Molina, F.J., Llave, E., Somoza, L., Fernandez-Puga, M.C., Maestro, A., Leon, R., Medialdea, T., Barnolas, A., Garcia, M., del Río, V.D., Fernandez-Salas, L.M., Vazquez, J.T., Lobo, F., Dias, J.M.A., Rodero, J. and Gardner, J., 2003. Looking for clues to paleoceanographic imprints: A diagnosis of the Gulf of Cadiz contourite depositional systems. *Geology*, 31(1): 19-22.
- Hernández-Molina, F.J., Llave, E., Stow, D.A.V., Garcia, M., Somoza, L., Vazquez, J.T., Lobo, F.J., Maestro, A., del Río, V.D., Leon, R., Medialdea, T. and Gardner, J., 2006. The contourite depositional system of the Gulf of Cadiz: A sedimentary model related to the bottom current activity of the Mediterranean outflow water and its interaction with the continental margin. *Deep-Sea Research Part II-Topical Studies in Oceanography*, 53(11-13): 1420-1463.
- Hernández-Molina, F.J., Llave, E. and Stow, D.A.V., 2008. Continental Slope Contourites. In: M. Rebesco and A. Camerlenghi (Editors), *Contourites*. Developments in Sedimentology. Elsevier, pp. 379-408.
- Hernández-Molina, F.J., Paterlini, M., Violante, R., Marshall, P., de Isasi, M., Somoza, L. and Rebesco, M., 2009. Contourite depositional system on the Argentine Slope: An exceptional record of the influence of Antarctic water masses. *Geology*, 37(6): 507-510.
- Hernández-Molina, F.J., Llave, E., Preu, B., Ercilla, G., Fontan, A., Bruno, M., Serra, N., Gomiz, J.J., Brackenridge, R.E., Sierro, F.J., Stow, D.A.V., García, M., Juan, C., Sandoval, N. and Arnaiz, A., 2014a. Contourite processes associated with the Mediterranean Outflow Water after its exit from the Strait of Gibraltar: Global and conceptual implications. *Geology*, 42(3): 227-230.
- Hernández-Molina, F.J., Stow, D.A.V., Alvarez-Zarikian, C., Acton, G., Bahr, A., Balestra, B., Ducassou, E., Flood, R.D., Flores, J.A., Furota, S., Grunert, P., Hodell, D.A., Jimenez-Espejo, F., Kim, J.K., Krissek, L., Kuroda, J., Li, B., Llave, E., Lofi, J., Lourens, L.J., Miller, M., Nanayama, F., Nishida, N., Richter, C., Roque, C., Pereira, H., Sanchez Goñi, M.F., Sierro, F.J., Singh, A.D., Sloss, C., Takahimizu, Y., Tzanova, A., Voelker, A., Williams, T. and Xuan, C., 2014b. Onset of Mediterranean outflow into the north Atlantic. *Science*, 344(6189): 1244-1250.
- Hernández-Molina, F.J., Sierro, F.J., Llave, E., Roque, C., Stow, D.A.V., Williams, T., Lofi, J., Van der Schee, M., Arnáiz, A., Ledesma, S., Rosales, C., Rodríguez-Tovar, F.J., Pardo-Igúzquiza, E. and

- Brackenridge, R.E., 2016a. Evolution of the gulf of Cadiz margin and southwest Portugal contourite depositional system: Tectonic, sedimentary and paleoceanographic implications from IODP expedition 339. *Marine Geology*, 377: 7-39.
- Hernández-Molina, F.J., Soto, M., Piola, A.R., Tomasini, J., Preu, B., Thompson, P., Badalini, G., Creaser, A., Violante, R.A., Morales, E., Paterlini, M. and De Santa Ana, H., 2016b. A contourite depositional system along the Uruguayan continental margin: Sedimentary, oceanographic and paleoceanographic implications. *Marine Geology*, 378: 333-349.
- Hernández-Molina, F.J., Wåhlin, A., Bruno, M., Ercilla, G., Llave, E., Serra, N., Rosón, G., Puig, P., Rebesco, M., Van Rooij, D., Roque, D., González-Pola, C., Sánchez, F., Gómez, M., Preu, B., Schwenk, T., Hanebuth, T.J.J., Sánchez Leal, R.F., García-Lafuente, J., Brackenridge, R.E., Juan, C., Stow, D.A.V. and Sánchez-González, J.M., 2016c. Oceanographic processes and morphosedimentary products along the Iberian margins: A new multidisciplinary approach. *Marine Geology*, 378: 127-156.
- Hovland, M. and Judd, A.G., 1988. Seabed Pockmarks and Seepages: Impact on Geology, Biology and the Marine Environment. Graham & Trotman Ltd., London, 293 pp.
- Izquierdo, A., Tejedor, L., Sein, D.V., Backhaus, J.O., Brandt, P., Rubino, A. and Kagan, B.A., 2001. Control Variability and Internal Bore Evolution in the Strait of Gibraltar: A 2-D Two-Layer Model Study. *Estuarine, Coastal and Shelf Science*, 53(5): 637-651.
- Jia, Y., 2000. Formation of an Azores Current Due to Mediterranean Overflow in a Modeling Study of the North Atlantic. *Journal of Physical Oceanography*, 30(9): 2342-2358.
- Judd, A.G. and Hovland, M., 1992. The evidence of shallow gas in marine sediments. *Continental Shelf Research*, 12(10): 1081-1095.
- Kaboth, S., Bahr, A., Reichert, G.-J., Jacobs, B. and Lourens, L.J., 2016. New insights into upper MOW variability over the last 150 kyr from IODP 339 Site U1386 in the Gulf of Cadiz. *Marine Geology*, 377: 136-145.
- Karl, H.A., Carlson, P.R. and Cacchione, D.A., 1983. Factors that Influence Sediment Transport at the Shelfbreak. In: D.J. Stanley and G.T. Moore (Editors), *The Shelfbreak: Critical Interface on Continental Margins*. SEPM Special Publication. SEPM Society for Sedimentary Geology, pp. 219-231.
- Kennett, J.P., 1982. *Marine Geology*. Prentice Hall, 813 pp.
- King, E.L., Bøe, R., Bellec, V.K., Rise, L., Skarðhamar, J., Ferré, B. and Dolan, M.F.J., 2014. Contour current driven continental slope-situated sandwaves with effects from secondary current processes on the Barents Sea margin offshore Norway. *Marine Geology*, 353: 108-127.
- Koulali, A., Ouazar, D., Tahayt, A., King, R.W., Vernant, P., Reilinger, R.E., McClusky, S., Mourabit, T., Davila, J.M. and Amraoui, N., 2011. New GPS constraints on active deformation along the Africa-Iberia plate boundary. *Earth and Planetary Science Letters*, 308(1-2): 211-217.
- Laberg, J.S. and Camerlenghi, A., 2008. The Significance of Contourites for Submarine Slope Stability. In: M. Rebesco and A. Camerlenghi (Editors), *Contourites. Developments in Sedimentology*. Elsevier, pp. 537-556.
- Laberg, J.S. and Vorren, T.O., 2000. The Trænadjupet Slide, offshore Norway — morphology, evacuation and triggering mechanisms. *Marine Geology*, 171(1): 95-114.
- Lamb, K.G., 2014. Internal Wave Breaking and Dissipation Mechanisms on the Continental Slope/Shelf. *Annual Review of Fluid Mechanics*, 46: 231-254.
- Lee, H. and Baraza, J., 1999. Geotechnical characteristics and slope stability in the Gulf of Cadiz. *Marine Geology*, 155: 173-190.
- Lee, H.J., Syvitski, J.P.M., Parker, G., Orange, D., Locat, J., Hutton, E.W.H. and Imran, J., 2002. Distinguishing sediment waves from slope failure deposits: field examples, including the 'Humboldt slide', and modelling results. *Marine Geology*, 192: 79-104.
- Llave, E., Hernandez-Molina, F.J., Somoza, L., Diaz-del Rio, V., Stow, D.A.V., Maestro, A. and Alveirinho Dias, J.M., 2001. Seismic stacking pattern of the Faro-Albufeira contourite system (Gulf of Cadiz): a Quaternary record of paleoceanographic and tectonic influences. *Marine Geophysical Researches*, 22: 487-508.

- Llave, E., Schönfeld, J., Hernandez-Molina, F.J., Mulder, T., Somoza, L., Diaz-del Rio, V. and Sanchez-Almazo, I., 2006. High-resolution stratigraphy of the Mediterranean outflow contourite system in the Gulf of Cadiz during the late Pleistocene: The impact of Heinrich events. *Marine Geology*, 277: 241-262.
- Llave, E., Hernandez-Molina, F.J., Somoza, L., Stow, D.A.V. and Diaz del Rio, G., 2007. Quaternary evolution of the contourite depositional system in the Gulf of Cadiz. In: A.R. Viana and M. Rebesco (Editors), *Economic and Palaeoceanographic Significance of Contourite Deposits*. Special Publication. Geological Society, London, pp. 49-79.
- Llave, E., Matias, H., Hernández-Molina, F., Ercilla, G., Stow, D. and Medialdea, T., 2011. Pliocene–Quaternary contourites along the northern Gulf of Cadiz margin: sedimentary stacking pattern and regional distribution. *Geo-Marine Letters*: 1-14.
- Lobo, F.J., Sánchez, R., González, R., Dias, J.M.A., Hernández-Molina, F.J., Fernández-Salas, L.M., Díaz del Río, V. and Mendes, I., 2004. Contrasting styles of the Holocene highstand sedimentation and sediment dispersal systems in the northern shelf of the Gulf of Cadiz. *Continental Shelf Research*, 24(4-5): 461-482.
- Lobo, F.J., Dias, J.M.A., Hernandez-Molina, F.J., Gonzalez, R., Fernandez-Salas, L.M. and Diaz-Del-Rio, V., 2005. Late Quaternary shelf-margin wedges and upper slope progradation in the Gulf of Cadiz margin (SW Iberian Peninsula). In: D.M. Hodgson and S.S. Flint (Editors), *Submarine Slope Systems: Processes and Products*. Geological Society, London, Special Publications, 244, pp. 7-25.
- Lobo, F.J. and Ridente, D., 2014. Stratigraphic architecture and spatio-temporal variability of high-frequency (Milankovitch) depositional cycles on modern continental margins: An overview. *Marine Geology*, 352: 215-247.
- Lobo, F.J., García, M., Luján, M., Mendes, I., Reguera, M.I. and Van Rooij, D., 2018. Morphology of the last subaerial unconformity on a shelf: insights into transgressive river avinement and incised valley occurrence in the Gulf of Cádiz. *Geo-Marine Letters*, 38(1): 33-45.
- Locat, J. and Lee, H.J., 2002. Submarine landslides: advances and challenges. *Canadian Geotechnical Journal*, 39(1): 193-212.
- Lofi, J., Voelker, A.H.L., Ducassou, E., Hernández-Molina, F.J., Sierro, F.J., Bahr, A., Galvani, A., Lourens, L.J., Pardo-Igúzquiza, E., Pezard, P., Rodríguez-Tovar, F.J. and Williams, T., 2016. Quaternary chronostratigraphic framework and sedimentary processes for the Gulf of Cadiz and Portuguese Contourite Depositional Systems derived from Natural Gamma Ray records. *Marine Geology*, 377: 40-57.
- Lonergan, L., Jamin, N.H., Jackson, C.A.L. and Johnson, H.D., 2013. U-shaped slope gully systems and sediment waves on the passive margin of Gabon (West Africa). *Marine Geology*, 337: 80-97.
- Løseth, H., Gading, M. and Wensaas, L., 2009. Hydrocarbon leakage interpreted on seismic data. *Marine and Petroleum Geology*, 26(7): 1304-1319.
- Louarn, E. and Morin, P., 2011. Antarctic Intermediate Water influence on Mediterranean Sea Water outflow. *Deep Sea Research Part I: Oceanographic Research Papers*, 58(9): 932-942.
- Maestro, A., Somoza, L., Medialdea, T., Talbot, C.J., Lowrie, A., Vázquez, J.T. and Díaz-del-Río, V., 2003. Large-scale slope failure involving Triassic and Middle Miocene salt and shale in the Gulf of Cádiz (Atlantic Iberian Margin). *Terra Nova*, 15(6): 380-391.
- Maldonado, A., Somoza, L. and Pallarés, L., 1999. The Betic orogen and the Iberian-African boundary in the Gulf of Cadiz: geological evolution (central North Atlantic). *Marine Geology*, 155: 9-43.
- Maldonado, A., Rodero, J., Pallarés, L., Pérez, L., Somoza, L., Medialdea, T., Hernández-Molina, F.J. and Lobo, F.J., 2003. Mapa Geológico de la Plataforma Continental Española y Zonas Adyacentes. Escala 1:200000. Instituto Geológico y Minero de España, Madrid, Spain.
- Marchès, E., Mulder, T., Cremer, M., Bonnel, C., Hanquiez, V., Gonthier, E. and Lecroart, P., 2007. Contourite drift construction influenced by capture of Mediterranean Outflow Water deep-sea current by the Portimao submarine canyon (Gulf of Cadiz, South Portugal). *Marine Geology*, 242(4): 247-260.

- Masson, D.G., Harbitz, C.B., Wynn, R.B., Pedersen, G. and Løvholt, F., 2006. Submarine landslides: processes, triggers and hazard prediction. *Philosophical Transactions of the Royal Society A: Mathematical, Physical and Engineering Sciences*, 364(1845): 2009-2039.
- McCave, I.N., 2017. Formation of sediment waves by turbidity currents and geostrophic flows: A discussion. *Marine Geology*, 390: 89-93.
- McCave, I.N. and Tucholke, B.E., 1986. Deep current-controlled sedimentation in the western North Atlantic. In: P.R. Vogt and B.E. Tucholke (Editors), *The Geology of North America, Volume M, The Western North Atlantic Region*. Geological Society of America, pp. 451-468.
- McIntyre, A., Kipp, N.G., Bé, A.W.H., Crowley, T., Kellogg, T., Gardner, J.V., Prell, W. and Ruddiman, W.F., 1976. Glacial North Atlantic 18,000 Years Ago: A CLIMAP Reconstruction. In: R.M. Cune and J.D. Hays (Editors), *Investigation of Late Quaternary Paleoceanography and Paleoclimatology*. GSA Memoirs. Geological Society of America, pp. 43-76.
- Medialdea, T., Vegas, R., Somoza, L., Vázquez, J.T., Maldonado, A., Díaz-del-Río, V., Maestro, A., Córdoba, D. and Fernández-Puga, M.C., 2004. Structure and evolution of the "Olistostrome" complex of the Gibraltar Arc in the Gulf of Cádiz (eastern Central Atlantic): evidence from two long seismic cross-sections. *Marine Geology*, 209(1-4): 173-198.
- Medialdea, T., Somoza, L., Pinheiro, L.M., Fernández-Puga, M.C., Vázquez, J.T., León, R., Ivanov, M.K., Magalhaes, V., Díaz-del-Río, V. and Vegas, R., 2009. Tectonics and mud volcano development in the Gulf of Cádiz. *Marine Geology*, 261(1-4): 48-63.
- Mestdagh, T., Lobo, F.J., Llave, E., Hernández-Molina, F.J. and Van Rooij, D., 2019. Review of the late Quaternary stratigraphy of the northern Gulf of Cadiz continental margin: New insights into controlling factors and global implications. *Earth-Science Reviews*, 198: 102944.
- Migeon, S., Savoye, B., Zanella, E., Mulder, T., Faugères, J.-C. and Weber, O., 2001. Detailed seismic-reflection and sedimentary study of turbidite sediment waves on the Var Sedimentary Ridge (SE France): significance for sediment transport and deposition and for the mechanisms of sediment-wave construction. *Marine and Petroleum Geology*, 18: 179-208.
- Millot, C., 2009. Another description of the Mediterranean Sea outflow. *Progress in Oceanography*, 52(2): 101-124.
- Miramontes, E., Garreau, P., Caillaud, M., Jouet, G., Pellen, R., Hernández-Molina, F.J., Clare, M.A. and Cattaneo, A., 2019. Contourite distribution and bottom currents in the NW Mediterranean Sea: Coupling seafloor geomorphology and hydrodynamic modelling. *Geomorphology*, 333: 43-60.
- Morton, R.A. and Suter, J.R., 1996. Sequence Stratigraphy and Composition of Late Quaternary Shelf-Margin Deltas, Northern Gulf of Mexico. *AAPG Bulletin*, 80(4): 505-530.
- Mougenot, D., Boillot, G. and Rehault, J.-P., 1983. Prograding Shelfbreak Types on Passive Continental Margins: Some European Examples. In: D.J. Stanley and G.T. Moore (Editors), *The Shelfbreak: Critical Interface on Continental Margins*. SEPM Special Publication. SEPM Society for Sedimentary Geology, pp. 61-77.
- Mulder, T., Voisset, M., Lecroart, P., Le Drezen, E., Gonthier, E., Hanquiez, V., Faugères, J.C., Habgood, E., Hernández-Molina, F.J., Estrada, F., Llave-Barranco, E., Poirier, D., Gorini, C., Fuchey, Y., Voelker, A., Freitas, P., Sanchez, F.L., Fernandez, L.M., Kenyon, N.H. and Morel, J., 2003. The Gulf of Cadiz: an unstable giant contourite levee. *Geo-Marine Letters*, 23(1): 7-18.
- Mulder, T., Gonthier, E., Lecroart, P., Hanquiez, V., Marches, E. and Voisset, M., 2009. Sediment failures and flows in the Gulf of Cadiz (eastern Atlantic). *Marine and Petroleum Geology*, 26(5): 660-672.
- Nelson, C.H., Baraza, J. and Maldonado, A., 1993. Mediterranean undercurrent sandy contourites, Gulf of Cadiz, Spain. *Sedimentary Geology*, 82: 103-131.
- Nelson, C.H., Baraza, J., Maldonado, A., Rodero, J., Escutia, C. and Barber, J.H., 1999. Influence of the Atlantic inflow and Mediterranean outflow currents on Late Quaternary sedimentary facies of the Gulf of Cadiz continental margin. *Marine Geology*, 155(1-2): 99-129.
- Normandeau, A., Campbell, D.C. and Cartigny, M.J.B., 2019. The influence of turbidity currents and contour currents on the distribution of deep-water sediment waves offshore eastern Canada. *Sedimentology*, 66(5): 1746-1767.

- Normark, W.R., Hess, G.R., Stow, D.A.V. and Bowen, A.J., 1980. Sediment waves on the Monterey fan levee: preliminary physical interpretation. *Marine Geology*, 37: 1-18.
- O'Grady, D.B., Syvitski, J.P.M., Pratson, L.F. and Sarg, J.F., 2000. Categorizing the morphologic variability of siliciclastic passive continental margins. *Geology*, 28(3): 207-210.
- Palomino, D., López-González, N., Vázquez, J.-T., Fernández-Salas, L.-M., Rueda, J.-L., Sánchez-Leal, R. and Díaz-del-Río, V., 2016. Multidisciplinary study of mud volcanoes and diapirs and their relationship to seepages and bottom currents in the Gulf of Cádiz continental slope (northeastern sector). *Marine Geology*, 378: 196-212.
- Peliz, A., Dubert, J., Marchesiello, P. and Teles-Machado, A., 2007. Surface circulation in the Gulf of Cadiz: Model and mean flow structure. *Journal of Geophysical Research*, 112: C11015.
- Peliz, A., Marchesiello, P., Santos, A.M.P., Dubert, J., Teles-Machado, A., Marta-Almeida, M. and Le Cann, B., 2009. Surface circulation in the Gulf of Cadiz: 2. Inflow-outflow coupling and the Gulf of Cadiz slope current. *Journal of Geophysical Research*, 114: C03011.
- Pichon, A., Morel, Y., Baraille, R. and Quaresma, L.S., 2013. Internal tide interactions in the Bay of Biscay: Observations and modelling. *Journal of Marine Systems*, 109-110: S26-S44.
- Pickering, K.T. and Hiscott, R.N., 2016. Deep marine systems: processes, deposits, environments, tectonics and sedimentation. Wiley & American Geophysical Union, 657 pp.
- Pinheiro, L.M., Song, H., Ruddick, B., Dubert, J., Ambar, I., Mustafa, K. and Bezerra, R., 2010. Detailed 2-D imaging of the Mediterranean outflow and meddies off Iberia from multichannel seismic data. *Journal of Marine Systems*, 79(1-2): 89-100.
- Pitman, W.C. and Golovchenko, X., 1983. The Effect of Sealevel Change on the Shelfedge and Slope of Passive Margins. In: D.J. Stanley and G.T. Moore (Editors), *The Shelfbreak: Critical Interface on Continental Margins*. SEPM Special Publication. SEPM Society for Sedimentary Geology, pp. 41-58.
- Porębski, S.J. and Steel, R.J., 2003. Shelf-margin deltas: their stratigraphic significance and relation to deepwater sands. *Earth-Science Reviews*, 62(3-4): 283-326.
- Posamentier, H.W. and Allen, G.P., 1993. Variability of the sequence stratigraphic model: effects of local basin factors. *Sedimentary Geology*, 86(1): 91-109.
- Prather, B.E., O'Byrne, C., Pirmez, C. and Sylvester, Z., 2017. Sediment partitioning, continental slopes and base-of-slope systems. *Basin Research*, 29(3): 394-416.
- Pratson, L.F., Nittrouer, C.A., Wiberg, P.L., Steckler, M.S., Swenson, J.B., Cacchione, D.A., Karson, J.A., Murray, A.B., Wolinsky, M.A., Gerber, T.P., Mullenbach, B.L., Spinelli, G.A., Fulthorpe, C.S., O'Grady, D.B., Parker, G., Driscoll, N.W., Burger, R.L., Paola, C., Orange, D.L., Field, M.E., Friedrichs, C.T. and Fedele, J.J., 2007. Seascape Evolution on Clastic Continental Shelves and Slopes. In: C.A. Nittrouer, J.A. Austin, M.E. Field, J.H. Kravitz, J.P.M. Syvitski and P.L. Wiberg (Editors), *Continental Margin Sedimentation: From Sediment Transport to Sequence Stratigraphy*. International Association of Sedimentologists Special Publication Number 37. Blackwell Publishing Ltd, pp. 339-380.
- Preu, B., Hernandez-Molina, F.J., Violante, R., Piola, A.R., Paterlini, C.M., Schwenk, T., Voigt, I., Krastel, S. and Spiess, V., 2013. Morphosedimentary and hydrographic features of the northern Argentine margin: The interplay between erosive, depositional and gravitational processes and its conceptual implications. *Deep-Sea Research Part I-Oceanographic Research Papers*, 75: 157-174.
- Price, J., Baringer, M.O., Lueck, R.G., Johnson, G.C., Ambar, I., Parrilla, G., Cantos, A., Kennelly, M.A. and Sanford, T.B., 1993. Mediterranean Outflow Mixing and Dynamics. *Science*, 259: 1277-1282.
- Quaresma, L.S. and Pichon, A., 2013. Modelling the barotropic tide along the West-Iberian margin. *Journal of Marine Systems*, 109-110: S3-S25.
- Rebesco, M., Hernández-Molina, F.J., Van Rooij, D. and Wåhlin, A., 2014. Contourites and associated sediments controlled by deep-water circulation processes: State-of-the-art and future considerations. *Marine Geology*, 352(0): 111-154.


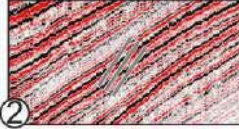

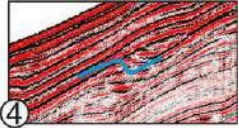
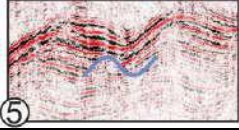
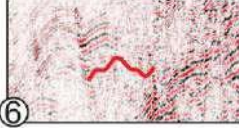
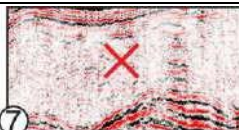
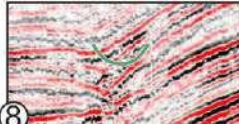
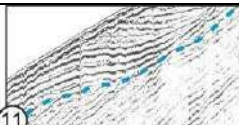
- Reiche, S., Hübscher, C., Brenner, S., Betzler, C. and Hall, J.K., 2018. The role of internal waves in the late Quaternary evolution of the Israeli continental slope. *Marine Geology*, 406: 177-192.
- Ribó, M., Puig, P., Muñoz, A., Lo Iacono, C., Masqué, P., Palanques, A., Acosta, J., Guillén, J. and Gómez Ballesteros, M., 2016. Morphobathymetric analysis of the large fine-grained sediment waves over the Gulf of Valencia continental slope (NW Mediterranean). *Geomorphology*, 253: 22-37.
- Richez, C., 1994. Airborne synthetic aperture radar tracking of internal waves in the Strait of Gibraltar. *Progress in Oceanography*, 33(2): 93-159.
- Ritchie, B.D., Gawthorpe, R.L. and Hardy, S., 2004. Three-Dimensional Numerical Modeling of Deltaic Depositional Sequences 2: Influence of Local Controls. *Journal of Sedimentary Research*, 74(2): 221-238.
- Rodero, J., Pallarés, L. and Maldonado, A., 1999. Late Quaternary seismic facies of the Gulf of Cadiz Spanish margin: depositional processes influenced by sea-level change and tectonic controls. *Marine Geology*, 155: 131-156.
- Rogerson, M., Colmenero-Hidalgo, E., Levine, R.C., Rohling, E.J., Voelker, A.H.L., Bigg, G.R., Schönfeld, J., Cacho, I., Sierro, F.J., Löwemark, L., Reguera, M.I., de Abreu, L. and Garrick, K., 2010. Enhanced Mediterranean-Atlantic exchange during Atlantic freshening phases. *Geochemistry Geophysics Geosystems*, 11(8): Q08013.
- Roque, C., Duarte, H., Terrinha, P., Valadares, V., Noiva, J., Cachão, M., Ferreira, J., Legoinha, P. and Zitellini, N., 2012. Pliocene and Quaternary depositional model of the Algarve margin contourite drifts (Gulf of Cadiz, SW Iberia): Seismic architecture, tectonic control and paleoceanographic insights. *Marine Geology*, 303–306: 42-62.
- Roque, D., Parras-Berrocal, I., Bruno, M., Sánchez-Leal, R. and Hernández-Molina, F.J., 2019. Seasonal variability of intermediate water masses in the Gulf of Cadiz: implications of the Antarctic and Subarctic seesaw model. *Ocean Sci. Discuss.*, 2019: 1-32.
- Rosenbaum, G., Lister, G.S. and Duboz, C., 2002. Relative motions of Africa, Iberia and Europe during Alpine orogeny. *Tectonophysics*, 359: 117-129.
- Roveri, M., Flecker, R., Krijgsman, W., Lofi, J., Lugli, S., Manzi, V., Sierro, F.J., Bertini, A., Camerlenghi, A., De Lange, G., Govers, R., Hilgen, F.J., Hübscher, C., Meijer, P.T. and Stoica, M., 2014. The Messinian Salinity Crisis: Past and future of a great challenge for marine sciences. *Marine Geology*, 352: 25-58.
- Sánchez-Garrido, J.C., Sannino, G., Liberti, L., García Lafuente, J. and Pratt, L., 2011. Numerical modeling of three-dimensional stratified tidal flow over Camarinal Sill, Strait of Gibraltar. *Journal of Geophysical Research: Oceans*, 116(C12).
- Sánchez-Leal, R.F., Bellanco, M.J., Fernández-Salas, L.M., García-Lafuente, J., Gasser-Rubinat, M., González-Pola, C., Hernández-Molina, F.J., Pelegrí, J.L., Peliz, A., Relvas, P., Roque, D., Ruiz-Villarreal, M., Sammartino, S. and Sánchez-Garrido, J.C., 2017. The Mediterranean Overflow in the Gulf of Cadiz: A rugged journey. *Science Advances*, 3(11).
- Schlitzer, R., 2017. Ocean Data View, odv.awi.de.
- Schmitz, W.J. and McCartney, M.S., 1993. On the North Atlantic Circulation. *Reviews of Geophysics*, 31(1): 29-49.
- Serra, N. and Ambar, I., 2002. Eddy generation in the Mediterranean undercurrent. *Deep Sea Research Part II: Topical Studies in Oceanography*, 49(19): 4225-4243.
- Shanmugam, G., 2006. Deep-Water Processes and Facies Models: Implications for Sandstone Petroleum Reservoirs. *Handbook of Petroleum Exploration and Production*. Elsevier, Amsterdam, 496 pp.
- Shanmugam, G., 2013. Modern internal waves and internal tides along oceanic pycnoclines: Challenges and implications for ancient deep-marine baroclinic sands. *AAPG Bulletin*, 97(5): 799-843.
- Shanmugam, G., 2018. Slides, Slumps, Debris Flows, Turbidity Currents, and Bottom Currents: Implications, Reference Module in Earth Systems and Environmental Sciences. Elsevier.
- Shepard, F.P., 1981. Submarine Canyons: Multiple Causes and Long-time Persistence. *Aapg Bulletin*, 65(6): 1062-1077.


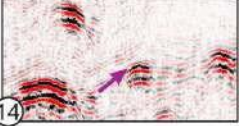
- Shumaker, L.E., Jobe, Z.R. and Graham, S.A., 2017. Evolution of submarine gullies on a prograding slope: Insights from 3D seismic reflection data. *Marine Geology*, 393: 35-46.
- Somoza, L., Hernandez-Molina, F.J., De Andres, J.R. and Rey, J., 1997. Continental shelf architecture and sea-level cycles: Late Quaternary high-resolution stratigraphy of the Gulf of Cadiz, Spain. *Geo-Marine Letters*, 17: 133-139.
- Srivastava, S.P., Schouten, H., Roest, W.R., Klitgord, K.D., Kovacs, L.C., Verhoef, J. and Macnab, R., 1990. Iberian plate kinematics: a jumping plate boundary between Eurasia and Africa. *Nature*, 344: 756-759.
- Steel, R.J., Carvajal, C., Petter, A.L. and Uroza, C., 2008. Shelf and Shelf-Margin Growth in Scenarios of Rising and Falling Sea Level. In: G.J. Hampson, R.J. Steel, P.M. Burgess and R.W. Dalrymple (Editors), *Recent Advances in Models of Siliciclastic Shallow-Marine Stratigraphy*. SEPM Special Publication. SEPM Society for Sedimentary Geology, pp. 47-71.
- Stow, D.A.V., Hernandez-Molina, F.J., Llave, E., Sayago-Gil, M., del Rio, V.D. and Branson, A., 2009. Bedform-velocity matrix: The estimation of bottom current velocity from bedform observations. *Geology*, 37(4): 327-330.
- Stow, D.A.V., Hernandez-Molina, F.J., Alvarez Zarikian, C.A. and Expedition 339 Scientists, 2013. Proc. IODP, 339. Integrated Ocean Drilling Program Management International, Tokyo.
- Sultan, N., Cochonat, P., Canals, M., Cattaneo, A., Dennielou, B., Hafliðason, H., Laberg, J.S., Long, D., Mienert, J., Trincardi, F., Urgeles, R., Vorren, T.O. and Wilson, C.K., 2004. Triggering mechanisms of slope instability processes and sediment failures on continental margins: a geotechnical approach. *Marine Geology*, 213: 291-321.
- Talling, P.J., Masson, D.G., Sumner, E.J. and Malgesini, G., 2012. Subaqueous sediment density flows: Depositional processes and deposit types. *Sedimentology*, 59(7): 1937-2003.
- Terrinha, P., Matias, L., Vicente, J., Duarte, J., Luís, J., Pinheiro, L., Lourenço, N., Diez, S., Rosas, F., Magalhães, V., Valadares, V., Zitellini, N., Roque, C. and Víctor, L.M., 2009. Morphotectonics and strain partitioning at the Iberia–Africa plate boundary from multibeam and seismic reflection data. *Marine Geology*, 267(3-4): 156-174.
- Urgeles, R., Cattaneo, A., Puig, P., Liqueste, C., De Mol, B., Amblàs, D., Sultan, N. and Trincardi, F., 2011. A review of undulated sediment features on Mediterranean prodeltas: distinguishing sediment transport structures from sediment deformation. *Marine Geophysical Research*, 32(1): 49-69.
- van Geen, A., Adkins, J.F., Boyle, E.A., Nelson, C.H. and Palanques, A., 1997. A 120-yr record of widespread contamination from mining of the Iberian pyrite belt. *Geology*, 25(4): 291-294.
- van Haren, H. and Puig, P., 2017. Internal wave turbulence in the Llobregat prodelta (NW Mediterranean) under stratified conditions: A mechanism for sediment waves generation? *Marine Geology*, 388: 1-11.
- Vanneste, M., Mienert, J. and Bunz, S., 2006. The Hinlopen Slide: A giant, submarine slope failure on the northern Svalbard margin, Arctic Ocean. *Earth and Planetary Science Letters*, 245(1-2): 373-388.
- Vanney, J.-R. and Stanley, D.J., 1983. Shelfbreak Physiography: An Overview. In: D.J. Stanley and G.T. Moore (Editors), *The Shelfbreak: Critical Interface on Continental Margins*. SEPM Special Publication. SEPM Society for Sedimentary Geology, pp. 1-24.
- Verdicchio, G. and Trincardi, F., 2008. Shallow-water contourites. In: M. Rebesco and A. Camerlenghi (Editors), *Contourites*. Developments in Sedimentology. Elsevier, pp. 409-433.
- Vlasenko, V., Sanchez Garrido, J.C., Stashchuk, N., Garcia Lafuente, J. and Losada, M., 2009. Three-Dimensional Evolution of Large-Amplitude Internal Waves in the Strait of Gibraltar. *Journal of Physical Oceanography*, 39(9): 2230-2246.
- Voelker, A.H.L., Lobreiro, S.M., Schonfeld, J., Cacho, I., Erlenkeuser, H. and Abrantes, F., 2006. Mediterranean outflow strengthening during northern hemisphere coolings: A salt source for the glacial Atlantic? *Earth and Planetary Science Letters*, 245(1-2): 39-55.
- Volkov, D.L. and Fu, L.-L., 2010. On the Reasons for the Formation and Variability of the Azores Current. *Journal of Physical Oceanography*, 40(10): 2197-2220.

- Wynn, R.B. and Stow, D.A.V., 2002. Classification and characterisation of deep-water sediment waves. *Marine Geology*, 192: 7-22.
- Wynn, R.B., Weaver, P.P.E., Ercilla, G., Stow, D.A.V. and Masson, D.G., 2000. Sedimentary processes in the Selvage sediment-wave field, NE Atlantic: new insights into the formation of sediment waves by turbidity currents. *Sedimentology*, 47(6): 1181-1197.
- Yin, S., Hernández-Molina, F.J., Zhang, W., Li, J., Wang, L., Ding, W. and Ding, W., 2019. The influence of oceanographic processes on contourite features: A multidisciplinary study of the northern South China Sea. *Marine Geology*, 415: 105967.
- Zecchin, M., Baradello, L., Brancolini, G., Donda, F., Rizzetto, F. and Tosi, L., 2008. Sequence stratigraphy based on high-resolution seismic profiles in the late Pleistocene and Holocene deposits of the Venice area. *Marine Geology*, 253(3-4): 185-198.
- Zitellini, N., Gracia, E., Matias, L., Terrinha, P., Abreu, M.A., DeAlteriis, G., Henriot, J.P., Danobeitia, J.J., Masson, D.G., Mulder, T., Ramella, R., Somoza, L. and Diez, S., 2009. The quest for the Africa-Eurasia plate boundary west of the Strait of Gibraltar. *Earth and Planetary Science Letters*, 280(1-4): 13-50.

<i>(sub-)units& surfaces</i>		<i>MIS</i>	<i>age (ka)</i>	<i>T/R</i>
U1	<i>mws1 (27 ka)</i>	MIS2 → present	27 → 0	T
U2	U2.1	MIS5 → MIS2	115 → 27	R
	U2.2 <i>mws2 (135 ka)</i>	MIS6 → MIS5	135 → 115	T
U3	U3.1	MIS7c → MIS6	200 → 135	R
	U3.2	MIS7d → MIS7c	225 → 200	T
	U3.3	MIS7e → MIS7d	240 → 225	R
	U3.4 <i>mws3 (262 ka)</i>	MIS8 → MIS7e	262 → 240	T
U4	U4.1	MIS9 → MIS8	310 → 262	R
	U4.2 <i>mws4 (335 ka)</i>	MIS10 → MIS9	335 → 310	T
U5	U5.1	MIS11 → MIS10	400 → 335	R
	U5.2 <i>mws5 (435 ka)</i>	MIS12 → MIS11	435 → 400	T

Table 1.

	<i>Morphological class</i>	<i>Characteristics</i>	<i>Position on upper slope</i>	<i>Stratigraphic position</i>
DEPOSITIONAL		- parallel continuous reflections (seaward dipping) - low amplitude - sheeted to wedge	- lower to middle part - east	mostly T sub-units
		- parallel continuous dipping reflections - moderate to high amplitude - sheeted to wedge (and locally infilling depressions)	- entire upper slope - east and west	mostly R sub-units
		- (sub)parallel continuous dipping refl. - moderate to high amplitude - slightly mounded (laterally extensive, locally onlapping depressions at base)	- middle to upper part - east and west	U1 (T)
		- wavy continuous reflections - asymmetric undulations - moderate to high amplitude	- lower part - east	U1 (T)
		- wavy continuous reflections - more symmetric undulations - moderate to high amplitude	- lower to middle part - east	mostly R
		- irregular-contorted discontinuous refl. - variable amplitude (low to high) - both large- and smaller-scale (local) features	- entire upper slope - east and west	mostly R
		- chaotic discontinuous reflections - very low amplitude to transparent - high-amplitude top (irregular) and base (irregular or smooth)	- lower part - east	U2.1 (R)
EROSIONAL		- linear, v-shaped erosional feature - downslope-oriented	- one example on middle part - east	U2.1 (R)
		- linear erosional depression - along slope-oriented - occur stacked (migrate upslope)	- upper part - east and west	U1 (T)
		- irregular erosional surface with deep and wide incisions, truncating refl. below - large-scale, overall downslope-oriented erosional system	- entire upper slope and (outer) shelf - east	within and at top U2.1 (R)
		- more regular to planar erosional surface - large-scale (covers large along slope elongated area)	- upper part slope and (outer) shelf - most pronounced west	top U2.1 (R) and sea floor
MIXED		- break-in-slope - associated with class 11 upslope and class 3 and 9 downslope	- upper part - west	sea floor

OTHER		<p>- transparent to very low-amplitude columnar body with chaotic reflections</p>	<p>- one example on middlepart - east</p>	<p>pierces U2 to U5</p>
		<p>- very high-amplitude spots - occur randomly, grouped at a specific surface, or within crests of undulations</p>	<p>- entire upper slope - east</p>	<p>both T and R sub-units</p>

Class	Interpretation	Dominant formation mechanism(s)
1	shelf-margin wedge (hemipelagic wedge)	hemipelagic sedimentation
2	shelf-margin wedge (shelf-margin delta)	sediment density (gravity) flows
3	plastered drift	along slope bottom currents
4	sediment waves	across-slope currents (internal waves/tides)
5		across-slope currents (turbidity currents)
6	slumps	subaqueous mass wasting
7	debrites	sediment density (gravity) flows
8	gully	turbidity currents
9	moat	along slope bottom currents
10	upperslope valley system	subaqueous mass wasting and erosion by turbidity currents
	outerslope valleys	fluvial incision on subaerially exposed shelf
11	erosion surface	along slope bottom currents
12	terrace	along slope bottom currents
13	diapir	response of lower density material (shale, marl or salt) to pressure variations
14	gas-related features (bright spots and pockmarks)	gas accumulation, migration and seepage

Research highlights

- Significant upper-slope morphological variability revealed off the Guadiana River
- Wide genetic diversity driven by along-/downslope processes, diapirism and gas flow
- Spatio-temporal patterns controlled by oceanographic variations and sediment supply

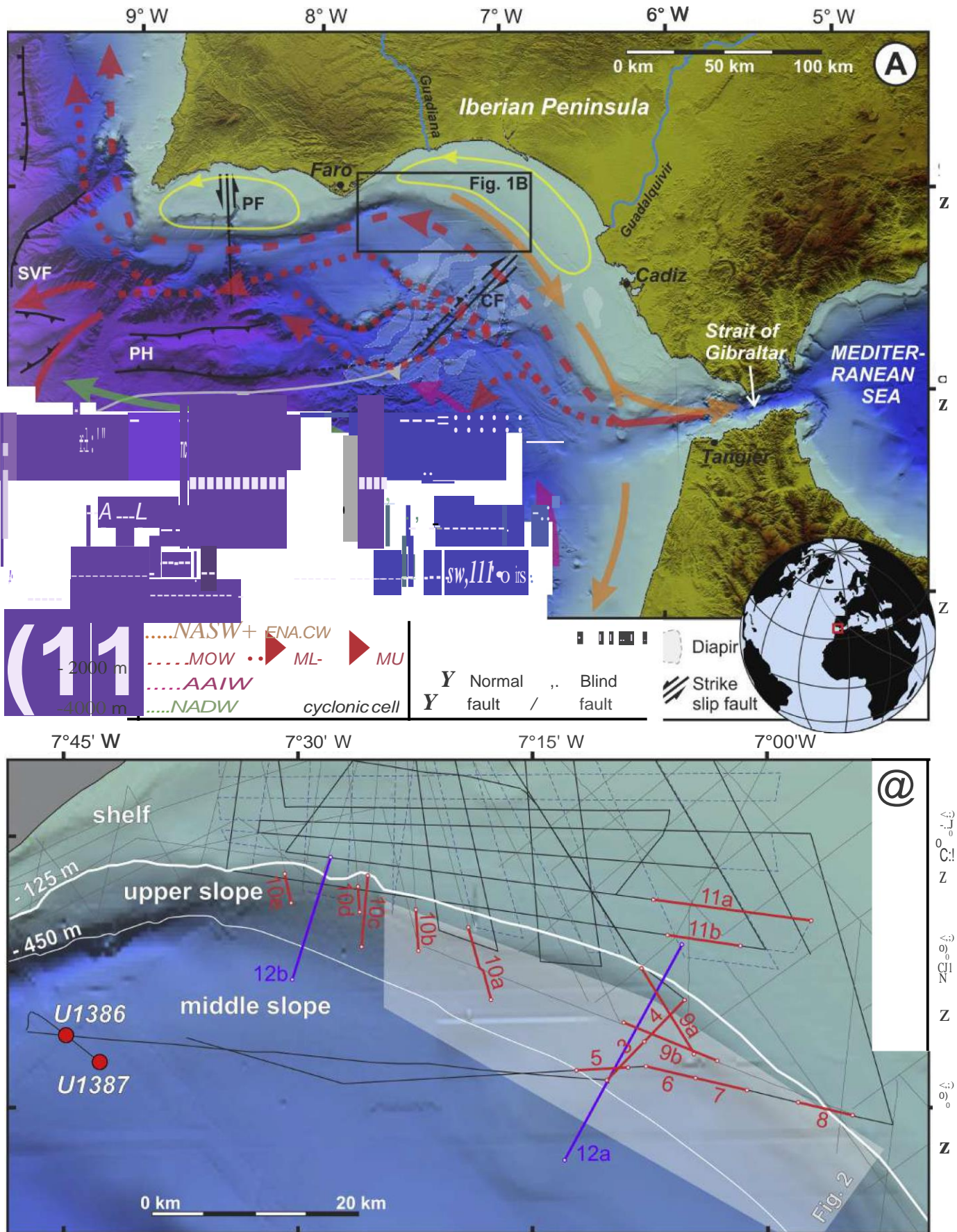


Figure 1

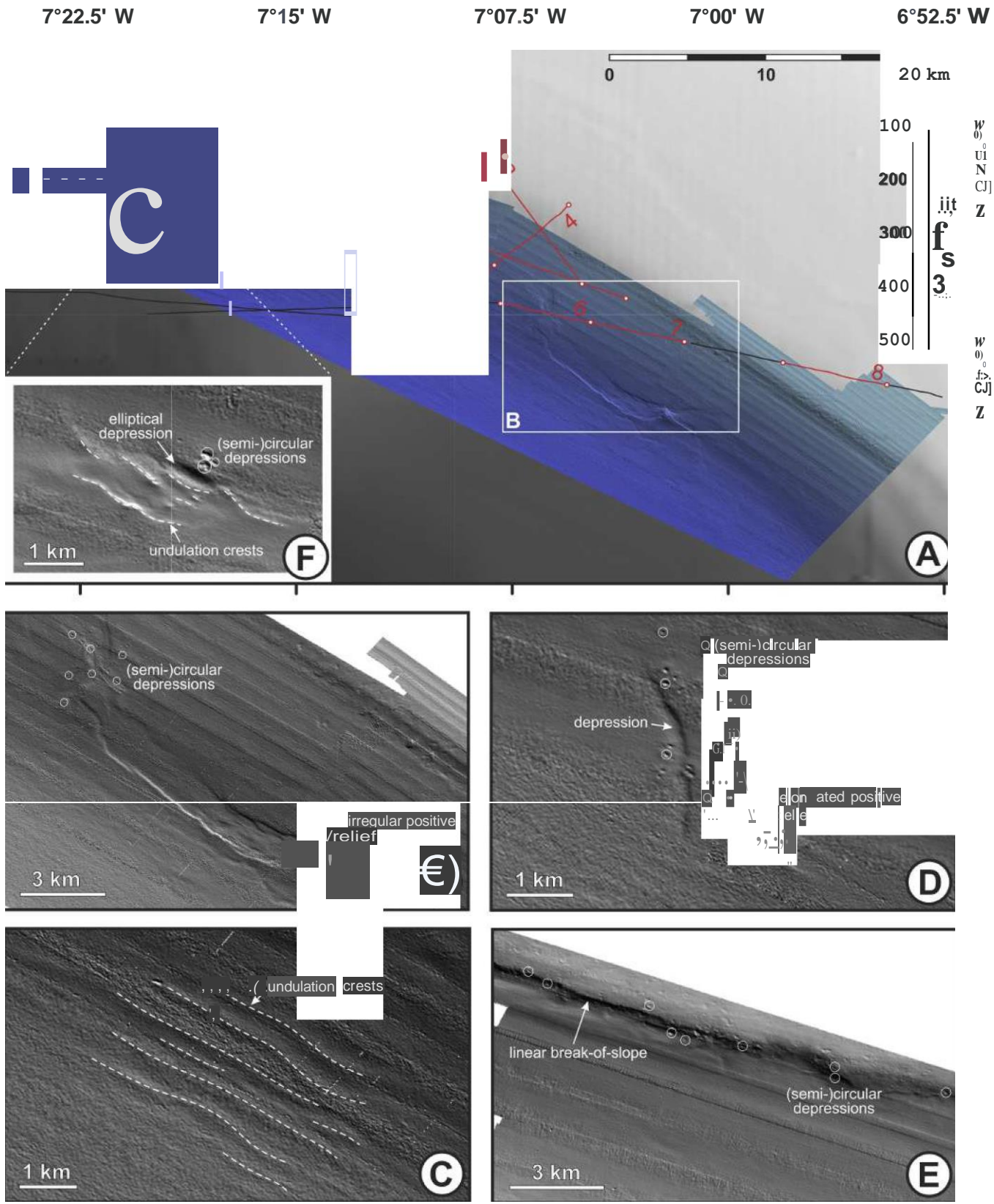


Figure 2

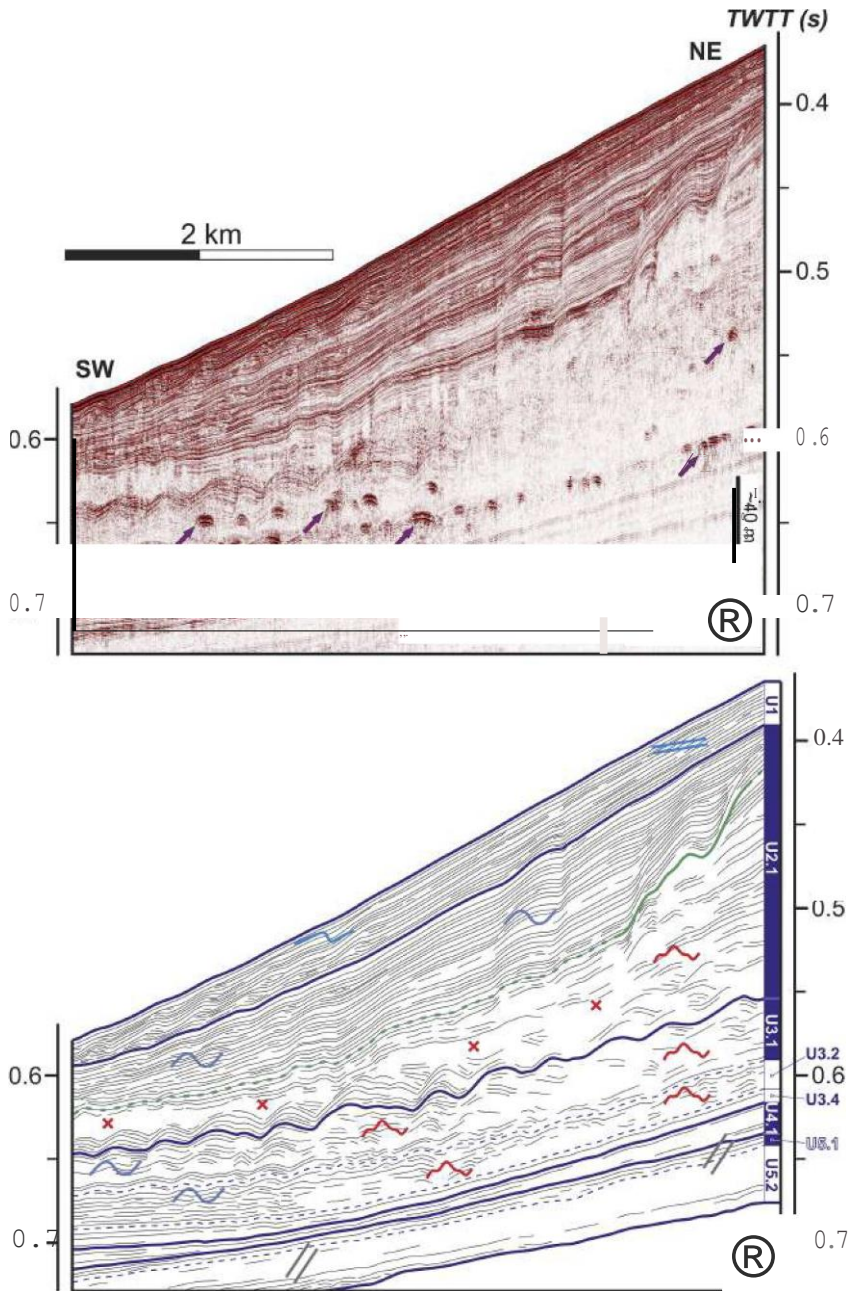


Figure 3

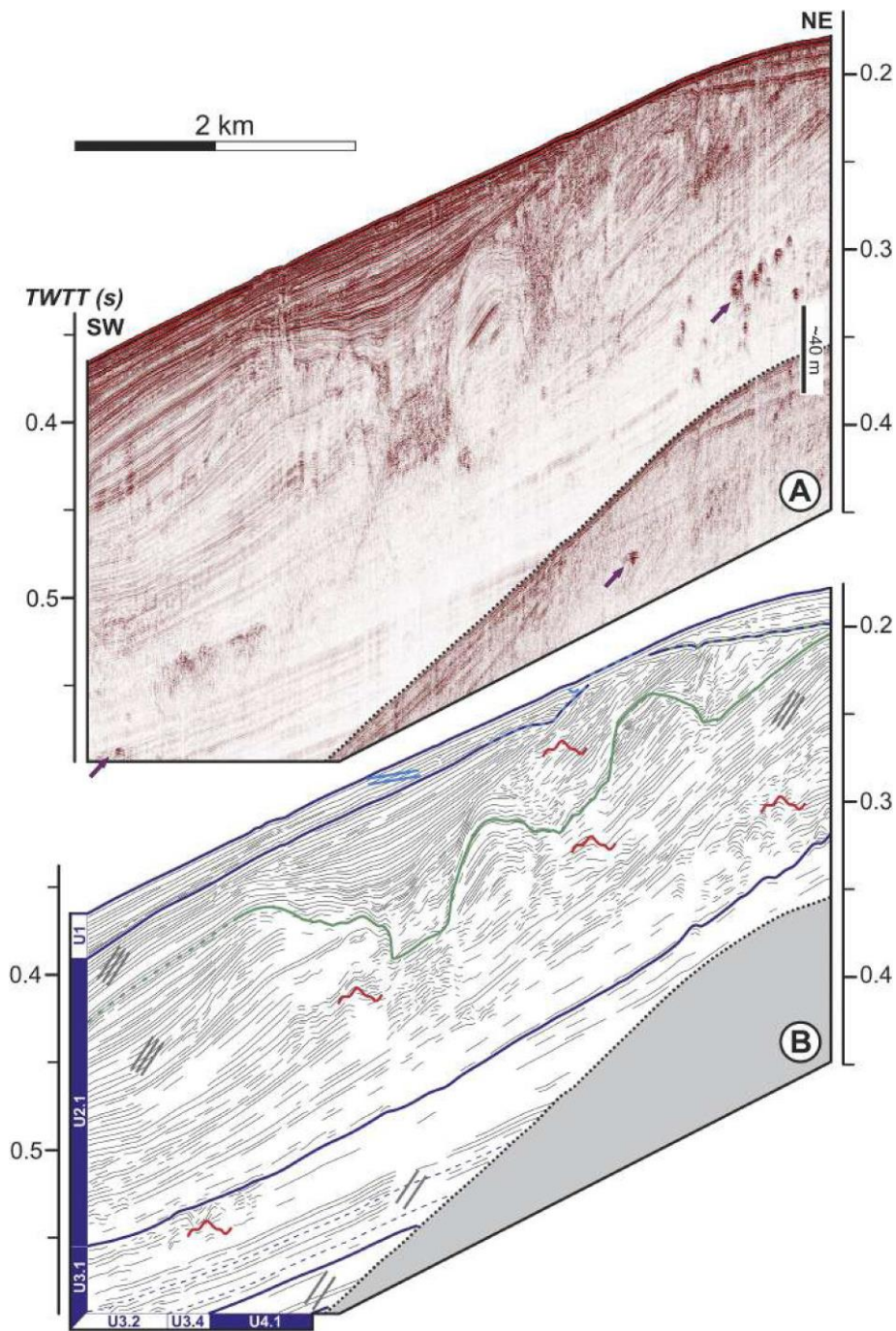
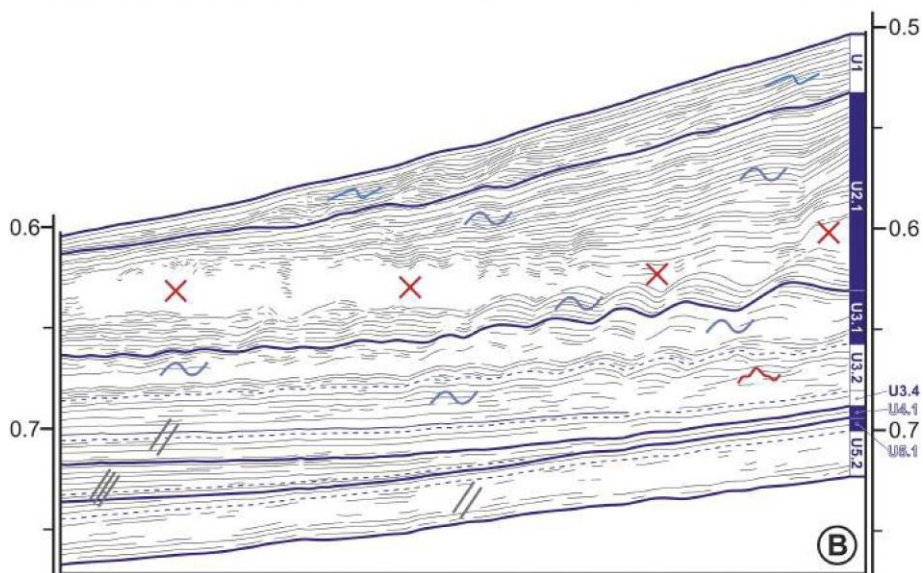
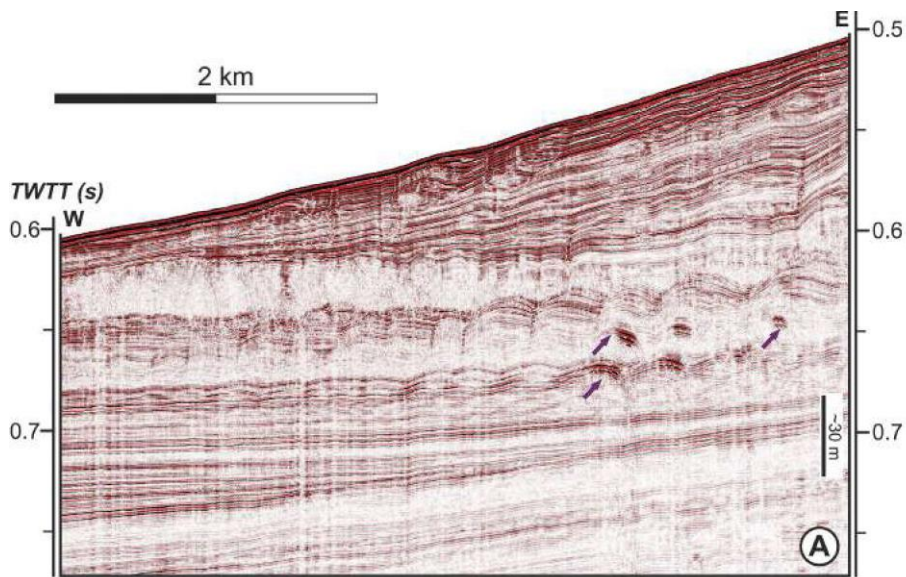


Figure 4



Figures

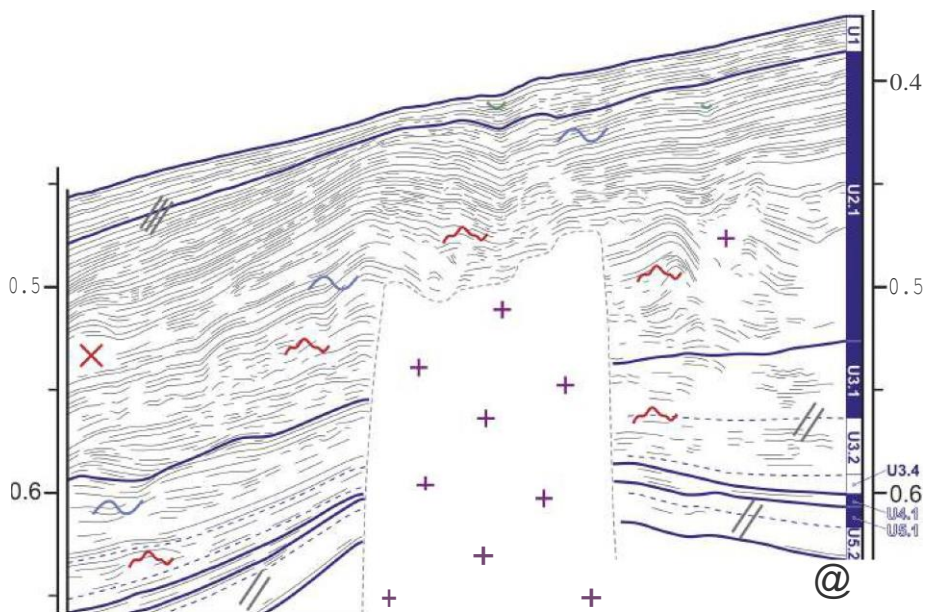
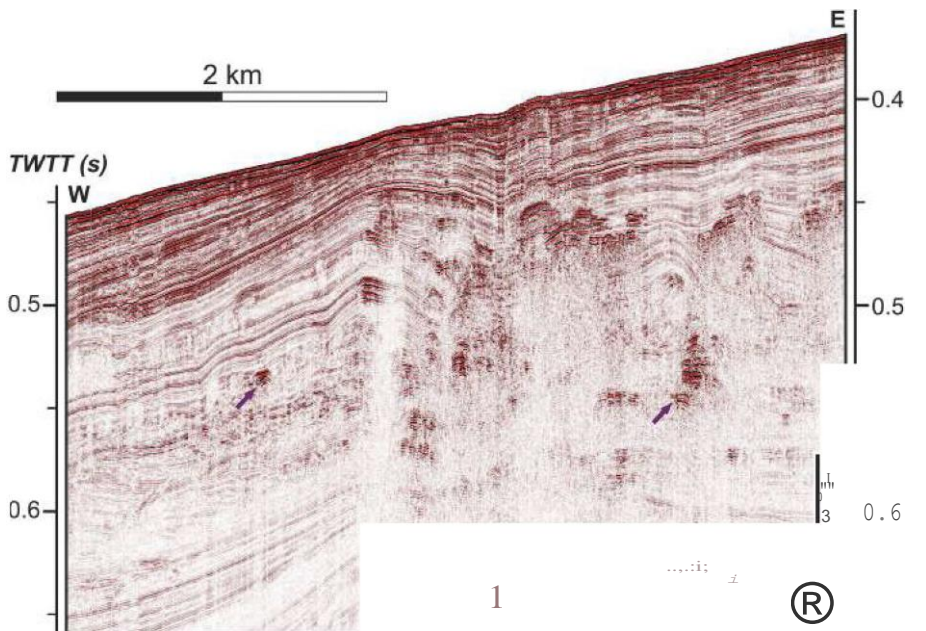


Figure 6

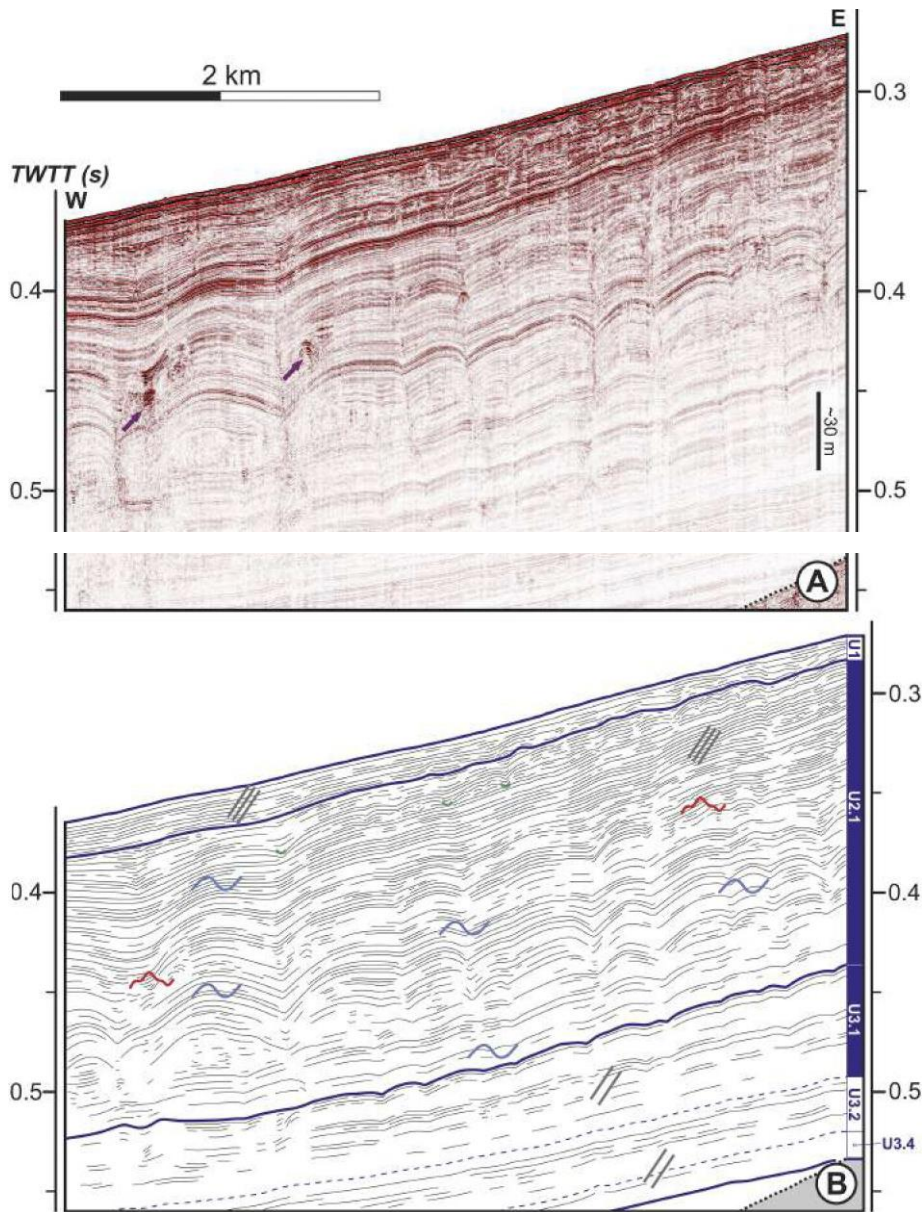
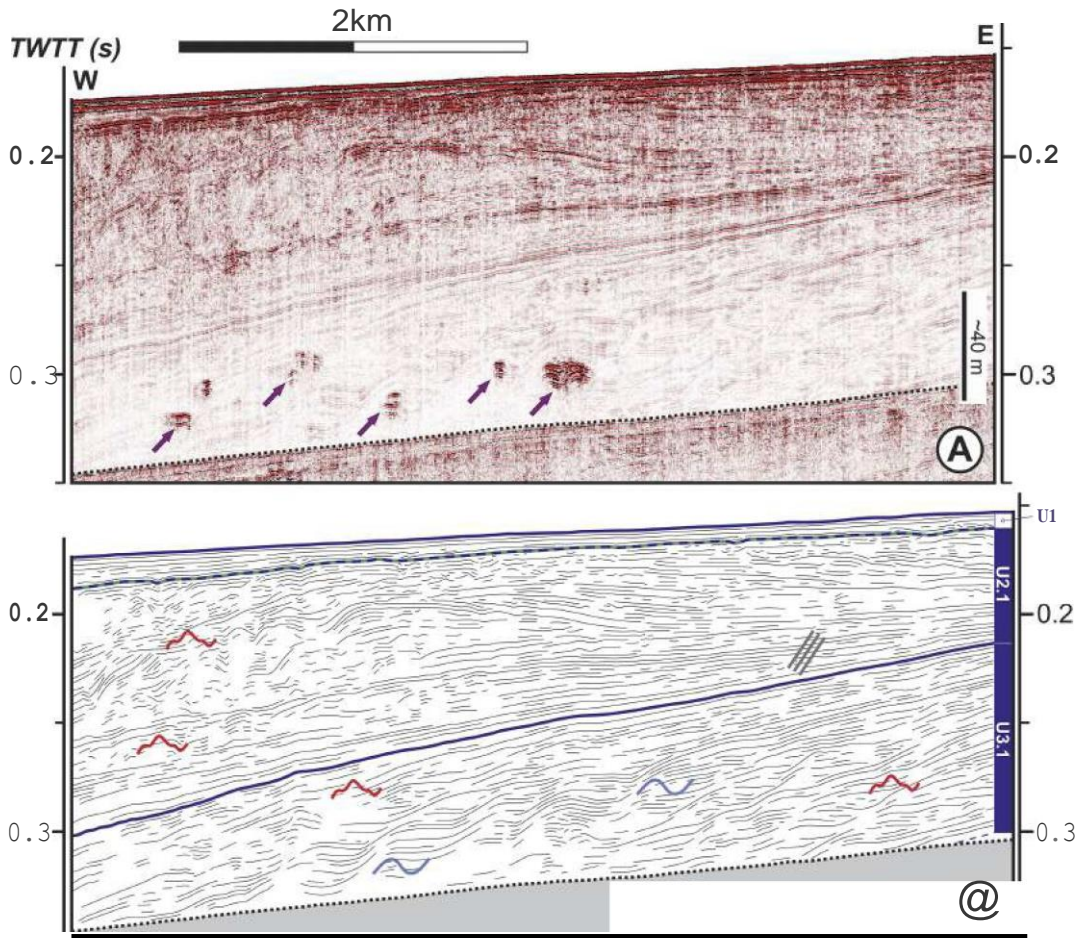


Figure 7



Figures

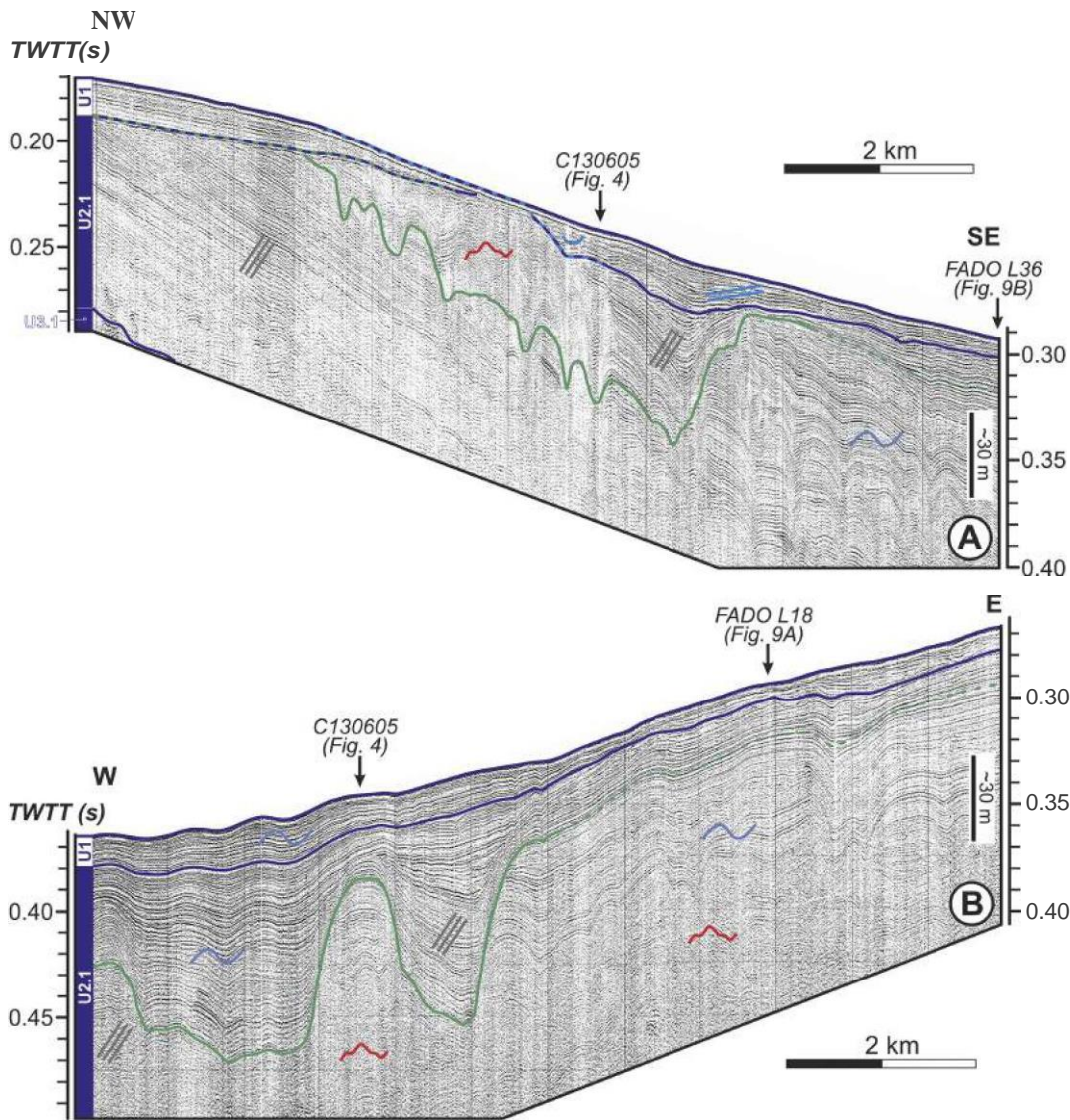


Figure 9

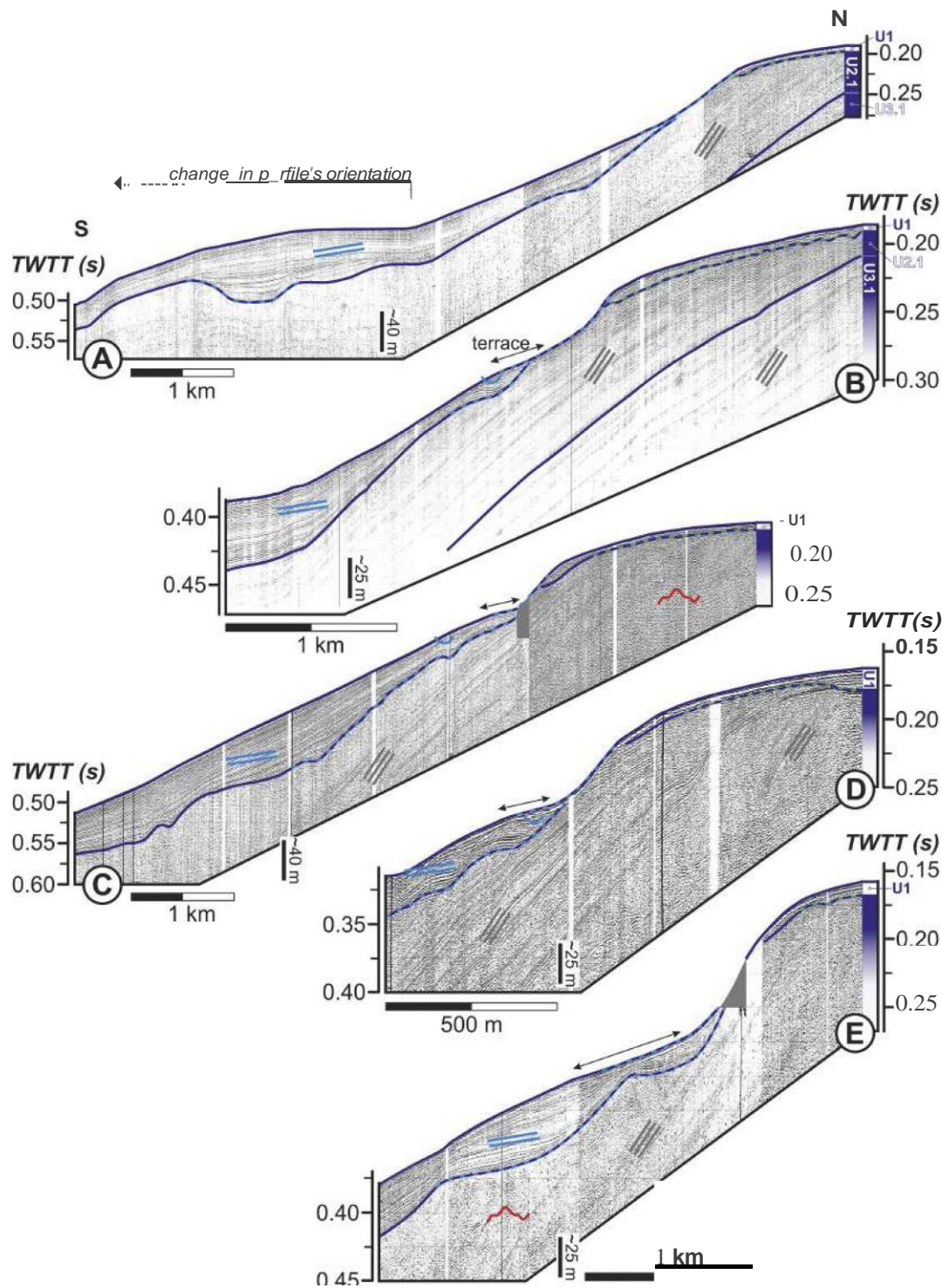


Figure 10

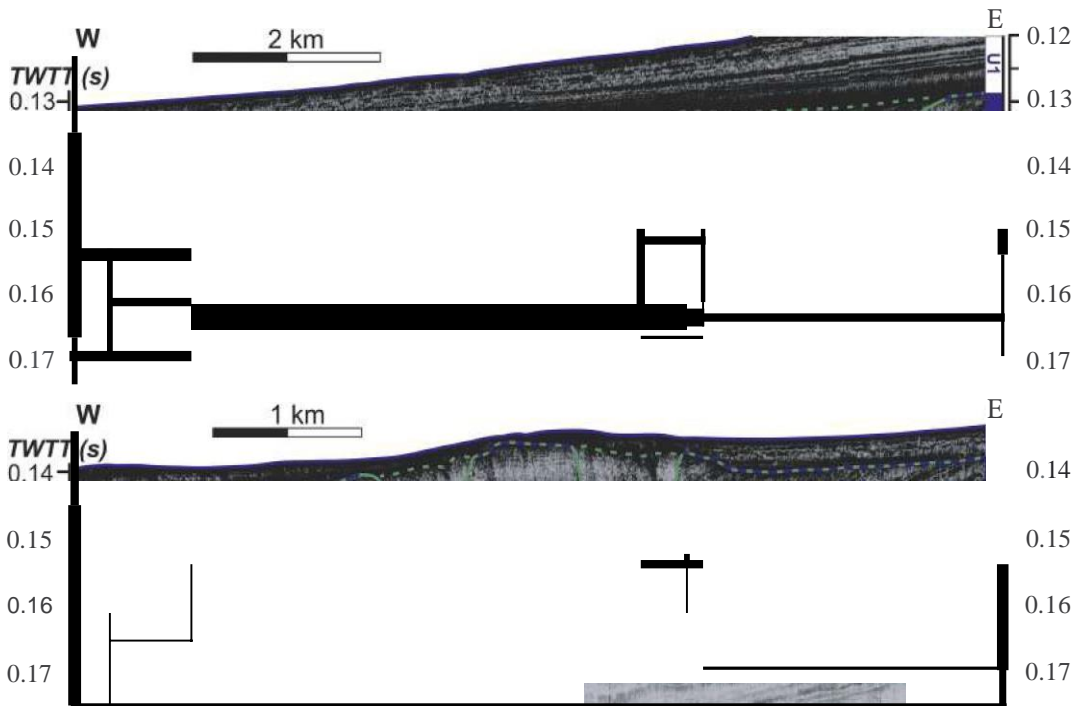
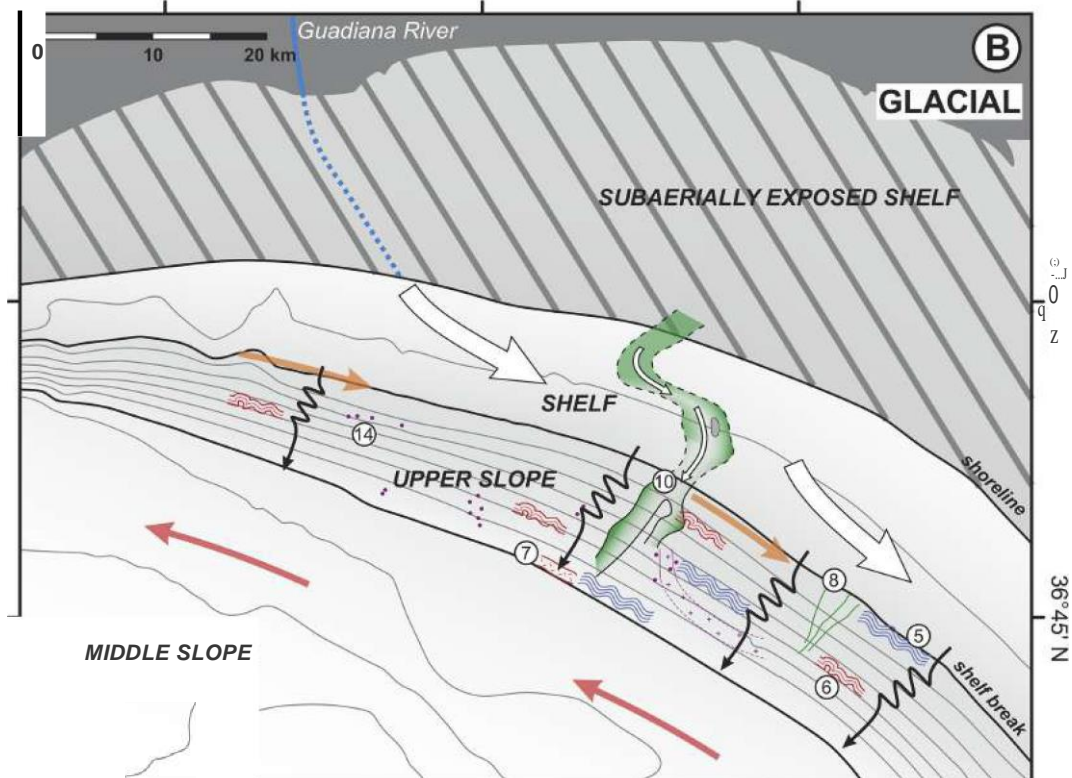
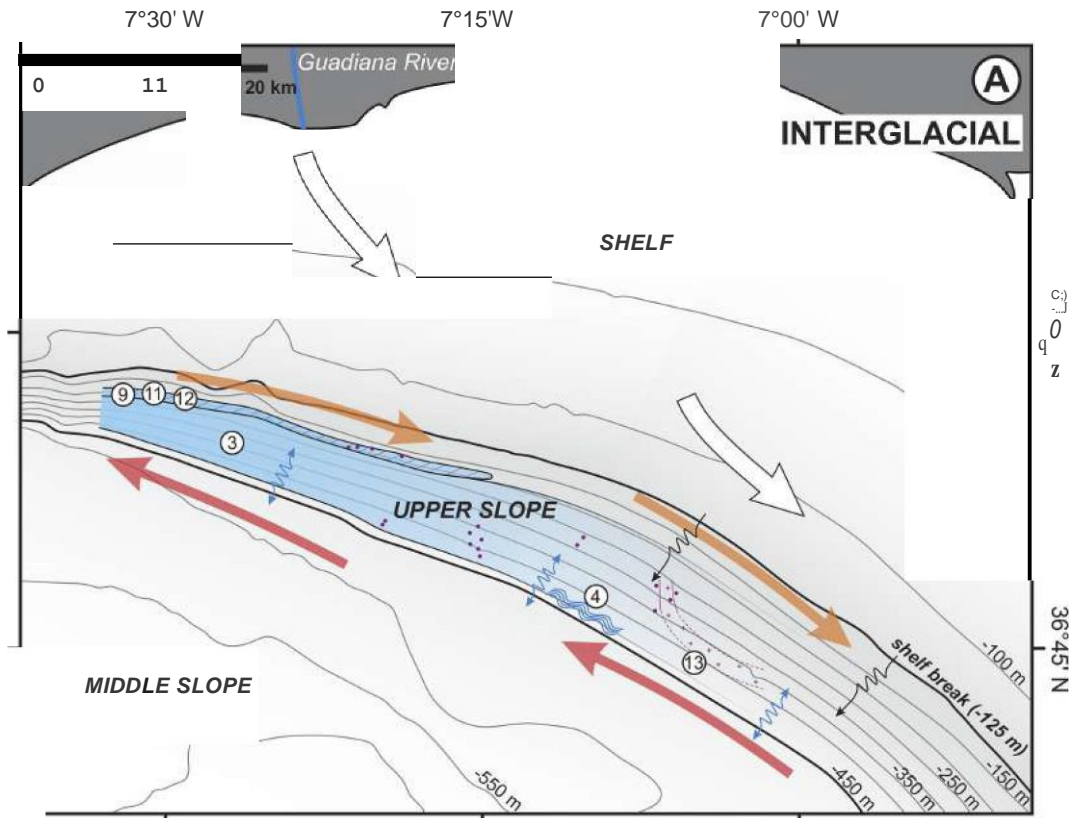


Figure 11



processes	===> terrigenous sediment input and dispersal		
_____ upperMOW ENACW (GCC)	internal waves	turbidity currents
products			
@ plastered drift	@ slumps	@ moat	@ terrace
© sediment waves (IW)	0 debrites	@ valley	@ diapir
Ⓡ sediment waves (TC)	@ gullies	@ erosion surface	<BJ pockmarks

Figure 13